Theme A: Loads and load models

THEME A

Loads and Load Models

Charges et modèles de charges

Lasten und Lastmodelle

Leere Seite
Blank page
Page vide

Bridge Load Models for Fatigue

Modèles de charge de fatigue pour des ponts en acier

Lastmodelle zur Untersuchung der Ermüdung von Stahlbrücken

Fred MOSES
Prof. of Civil Eng.
Case Western Reserve Univ.
Cleveland, OH, USA

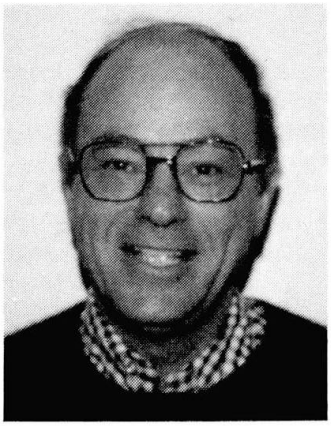

Fred Moses received a civil engineering degree from CUNY in 1960 and a PhD from Cornell in 1963. Since joining Case Institute, Professor Moses has been active in structural optimization and reliability with special applications to bridge and offshore structures including loading, safety analysis and system reliability studies.

SUMMARY

This study was performed to support new specifications for fatigue life design of steel bridges and also, the assessment of remaining fatigue life of existing steel bridges. A major part of the research included modelling truck loading and bridge stress response. Data was collected on truck weight distributions, dynamic response, lateral distribution analysis and stress spectra. A load model is proposed in order to predict bridge response. Data is used to calibrate the load model by describing each variable in terms of its coefficient of variation. An application of the load model to fatigue specifications is presented.

RÉSUMÉ

Cette étude a été effectuée dans le but de soutenir de nouvelles directives relatives à la conception à la fatigue de nouveaux ponts en acier, ainsi qu'à l'évaluation de la durée de vie restante des ponts existants. Une grande partie de la recherche a été consacrée au développement des modèles de charge de camion et à l'analyse des contraintes dans l'ouvrage. Des statistiques sur la distribution du poids des camions, ainsi que sur la réaction dynamique, la répartition transversale et les spectres de contrainte ont été rassemblées. Un modèle de charge est proposé dans le but de pouvoir prédire la réponse de l'ouvrage. Les données statistiques ont été utilisées pour établir ce modèle de charge en considérant le coefficient de variation de chacune des variables. Un exemple d'utilisation du modèle de charge pour l'étude de la résistance à la fatigue est présenté.

ZUSAMMENFASSUNG

Diese Studie wurde mit dem Ziel durchgeführt, neue Vorschriften über die Ermüdungsbemessung von Stahlbrücken und die Schätzung der Restlebensdauer bestehender Stahlbrücken aufzustellen. Der grösste Teil der Forschungsarbeit betrifft die Entwicklung von Lastmodellen zur Berücksichtigung des Schwerverkehrs und das Studium der in Brückenkonstruktionen auftretenden Spannungen. Daten wurden gesammelt zur statistischen Verteilung der Fahrzeuggewichte, zum dynamischen Verhalten von Brücken, zur Querverteilung der Lasten sowie zu den in Brücken vorkommenden Spannungsspektren. Ein Lastmodell wird vorgeschlagen, um die Reaktion einer Brücke vorhersagen zu können. Zur Kalibrierung dieses Modells wurden die Variationskoeffizienten aller vorgenannten Variablen verwendet. Ein Beispiel zeigt, wie das Lastmodell zur Untersuchung von Ermüdungsproblemen angewendet werden kann.

1. INTRODUCTION

The maintenance and safety of existing bridges is an important concern of all highway agencies. To assure adequate safety and to assist in assessing maintenance needs, highway bridges are periodically inspected, usually at 2-year intervals in the United States. In conjunction with such inspections, a safety rating is established by procedures given in the AASHTO *Manual for Maintenance Inspection of Bridges* [1]. The *Manual* presents detailed procedures for rating the strength capacity of steel bridges but does not give detailed procedures for assessing the safety with respect to fatigue. Instead, it suggests that the AASHTO *Standard Specifications for Highway Bridges* [2] be used as a guide in assessing fatigue strength.

The fatigue provisions in the *Specifications* were originally adopted before adequate information was available on the fatigue conditions in actual bridges. Therefore, these provisions do not reflect the fatigue conditions that actually occur. Instead, they combine an artificially high stress range with an artificially low number of stress cycles to produce a reasonable design. Furthermore, the fatigue provisions in the *Specifications* are presented in terms of allowable stresses and do not indicate how to calculate the remaining life of an existing bridge, which is needed in decisions regarding inspection, repair, rehabilitation, and replacement.

The objective of the present study is to develop practical fatigue evaluation procedures that:

1. Realistically reflect the actual fatigue conditions in highway bridges
2. Give an accurate estimate of the remaining fatigue life of a bridge and permit this estimate to be updated in the future to reflect changes in traffic conditions.
3. Provide consistent and reasonable levels of reliability.
4. Permit different levels of effort to reduce uncertainties and improve predictions of remaining life.
5. Apply consistently to both the evaluation of existing bridges and the design of new bridges.
6. Can be conveniently modified to reflect future research.
7. Are suitable for both the AASHTO Maintenance Manual [1] and Design Specifications [2].

2. FATIGUE LOAD MODEL

Fatigue life of steel bridges is primarily affected by the repetitive load cycles caused by passage of heavy vehicles. The stress ranges that occur at critical locations in actual bridges under normal traffic have been extensively measured. Results are usually reported in terms of effective stress range which is defined as the equivalent constant-amplitude stress range that provide the same fatigue damage as the variable-amplitude spectrum. The average effective stress range for some 215 histograms surveyed is 1.8 ksi [3]. The single highest effective stress range is 4.9 ksi and the next highest is 4.4 ksi. These data suggest that the peak stress range for histograms for steel girder or beam bridges is almost always below 10 ksi and that the effective stress range is almost always below 4.5 ksi (1 ksi = 6.89 Mpa).

Design stress ranges calculated by present AASHTO procedures are usually well above these measured stress ranges. Many factors contribute to the difference. Some of these result from the use in fatigue calculations of static-design procedures that are based on extreme conditions. Fatigue damage actually results from typical, or average, rather than extreme conditions. Specifically, the AASHTO live load design truck, the AASHTO lateral distribution factors, and the AASHTO impact factors are too conservative for fatigue calculations.

Many other factors that contribute to the difference between design and measured stresses are difficult to calculate and are conservatively ignored in design calculations. These include (1)

unintended composite action; (2) contributions to strength from nonstructural elements, such as parapets; (3) unintended partial end fixity at abutments; (4) catenary tension forces due to "frozen" joints or rigid end supports; (5) longitudinal distribution of moment; (6) direct transfer of load through the slab to the supports; and (7) direct transfer of load through the deck to supports in truss bridges. Although these factors are difficult to calculate, they consistently combine to produce actual stresses well below those calculated by normal procedures.

Average daily traffic volumes (ADT) of 120,000 are not unusual on major six-lane highways in large cities. The corresponding traffic volume in one direction is 60,000. About 10 percent of urban traffic is composed of trucks and about 75 percent of these trucks are in the shoulder lanes. Thus, the average daily truck traffic (ADTT) in the shoulder lane may exceed 4,500 in some cases. This truck volume applied over a 50-year life results in 82 million truck passages. Many bridges put into service in the 1930's are now 50 years old. In most cases, each truck passage causes one stress cycle, but in some cases it may cause more equivalent stress cycles. Thus, well over 100 million stress cycles, and perhaps as high as 300 million cycles, can occur in some bridges. The cyclic life categories used in selecting the AASHTO allowable fatigue stresses are generally well below this number, for example, 2 million cycles [2]. Thus, comparing the true situation to the specification shows lower effective stresses but a much higher number of cycles.

2.1 Concepts of Fatigue Safety

The concept of safety as applied to repetitive loads that cause fatigue damage is quite different from the concepts that are applied in strength design of a bridge with respect to maximum static (nonrepetitive) loads. For fatigue, many loading repetitions are required to produce a failure at some time in the future. Generally, all truck loading stresses, whether above or below the allowable stress range value, cause fatigue damage. The effects of fatigue loading on an existing bridge can best be defined in terms of the remaining safe fatigue life of the bridges. Similarly, the effects of fatigue loading on a new bridge can best be defined in terms of the total life of the bridge, although it may be convenient to use a permissible stress range corresponding to a desired design life to facilitate the reproportioning of members that do not have an adequate life. Safety factors can be applied in calculating the remaining or total life to assure that the actual life will exceed the calculated life with a desired degree of reliability.

2.2 Proposed Design or Evaluation Procedures

Several techniques have been proposed for fatigue design or evaluation procedures for various structural applications. These procedures are intended to realistically reflect the actual fatigue conditions that occur in the structure under consideration. Consequently, they generally involve three steps: (1) calculate the variable-amplitude stress spectrum caused by the actual loading, (2) relate this variable-amplitude stress spectrum to an equivalent or effective constant-amplitude stress by some cumulative damage approach, and (3) compare the resulting applied stress parameter with a fatigue strength (SN) curve to obtain the fatigue life. In many of the design procedures, probabilistic methods are used to define the degree of uncertainty in the calculations and to provide consistent levels of safety. These approaches are consistent with the probabilistic or reliability approaches used in various strength design codes. Factors of safety may be applied to the applied stress, the strength parameter and/or the design life.

The uncertainty in the calculated variable-amplitude stress spectrum depends on how accurately the loading can be defined and on how accurately stresses can be calculated from the loading. For highway bridges, truck traffic is the main fatigue loading and a gross weight histogram for such traffic is the most important parameter defining this loading. Therefore, most of the proposed procedures define a typical histogram or permit the use of an actual histogram for the site. The wheel spacings and distributions of the gross weights to various axles are also important

and are defined in most of the proposed procedures. Calculation of the stresses from the loading involves factors to account for lateral distribution, impact, and truck superpositions. These parameters are usually covered in some way in the proposed procedures.

Miner's linear cumulative damage law is used in almost all of the proposed procedures to relate variable-amplitude fatigue behavior to constant-amplitude behavior derived from lab test data. Although Miner's Law is often criticized by researchers, especially those dealing with special types of loadings, an extensive study of simulated bridge members showed that it is unbiased and that the scatter in predicting the life is not large. In this concept, a variable-amplitude spectrum is represented by an equivalent constant-amplitude stress cycle. This concept is carried one step further herein and uses an effective fatigue truck to represent typical truck traffic.

3. LOAD MODEL

A consistent load model is needed for fatigue design and evaluation procedures. Each variable must be identified and test data used to estimate the bias (mean to nominal value) and coefficient of variation (COV). Because the fatigue process is an averaging of damage accumulation, it is important that scatter emphasize site to site variation. For example, dynamic impact varies greatly with different vehicle types and gross weights. Hence, measured impacts at a site will have a large COV. But for that particular site the damage accumulation will not reflect this large scatter since the average damage per vehicle is of concern in computing the life. Thus, the mean impact is of greatest interest. The variation of this mean impact, however, from site to site is important since it greatly affects the estimate of accumulated damage per unit time interval.

3.1 Load Calculation

The true stress for any truck crossing depends on several variables and may be written as:

$$S_i = \frac{M_i}{S_x} = \frac{W_i g i m h}{S_x} \qquad (1)$$

where S_i is the nominal stress range on the attachment detail, M_i = maximum bending moment range of the i^{th} truck crossing event on the girder, W_i = i^{th} truck crossing gross vehicle weight, m = influence factor relating truck weight to maximum bending moment, i = impact amplification, g = lateral girder distribution (expressed as percent of gross span moment carried by a single member), h = account for closely spaced or multilane presence of vehicles which amplify the moment, and S_x = actual section modulus.

Equation 1 gives the stress range for the i^{th} truck crossing event. It relates to the design stress range through the selection of the section modulus, which is expressed using similar terms:

$$S_{XD} = \frac{\gamma W_D g_D i_D m_D h_D}{S_{rD}} \tag{2}$$

where γ is the reliability factor to be specified after calibration of the risk (this factor ensures an acceptable risk for the computed fatigue life of the member). W_D, g_D, i_D, m_D, h_D, are the specified nominal or design values of W, g, i, m, and h, respectively. S_{rD} is the design or allowable stress range. (This is obtained from the fatigue strength curves (SN curves) corresponding to expected lifetime total number of cycles the member is subjected). S_{XD} is the computed value of section. In general, the actual section modulus S_X is a random variable. S_{XD} and S_X are related by a random variable Z_X by:

$$S_X = Z_X S_{XD} \tag{3}$$

Z_X reflects the scatter in the true section modulus compared to nominal section modulus.

3.2 Damage Accumulation

According to Miner's rule the accumulated damage is:

$$D = \sum \frac{1}{N(S_i)} \tag{4}$$

where the sum is over each of the stress cycles S_i. $N(S_i)$ is the number of cycles to failure at a constant amplitude stress range of S_i. The fatigue curve may be described as the straight line log S vs. N curve written as:

$$NS^b = c \tag{5}$$

where the exponent b equals 3 for most welded attachments [3].

Substitution in Eq. 4 gives:

$$D = \frac{1}{c} \sum S_i^3 \tag{6}$$

Substituting Eqs. 1, 2, and 3 into Eq. 6 gives:

$$D = \frac{1}{c} \Sigma \left(\frac{W_i g m i h}{\gamma Z_x W_D g_D i_D m_D h_D} S_{rD} \right)^3 \tag{7}$$

$$= \frac{V}{c} \left(\frac{gmih}{\gamma Z_x W_D g_D i_D m_D h_D} S_{rD}\right)^3 \Sigma \frac{W_i^3}{V}$$

where V = number of trucks per year.

To simplify, let

$$W_{eq} = (\Sigma f(W_i) W_i^3)^{1/3} \tag{8}$$

where W_{eq} = equivalent fatigue truck weight, and $f(W_i)$ = percentage of trucks within weight interval W_i. Let:

$$V = ADTT(365)C \tag{9}$$

where V = volume, reflecting the total number of equivalent stress cycles in a year (a random variable), ADTT = average daily truck traffic in vehicles per day (a random variable), C = equivalent number of stress range cycles per truck crossing (a random variable).

Substituting Eqs. 8 and 9 into Eq. 7 gives:

$$D = \frac{1}{c} ADTT(365)C \left(\frac{W_{eq} gmih}{\gamma Z_x W_D g_D i_D m_D h_D} S_{rD}\right)^3 \tag{10}$$

Simplifying further gives:

$$c = N_T S_r^3 = N_T \left(\frac{S_r}{S_{rD}}\right)^3 S_{rD}^3 \tag{11}$$

where S_r is the true stress range (a random variable) from the SN curve corresponding to N_T number of stress cycles. N_T is a reference number of cycles and is deterministic. For convenience, it is chosen to be numerically equal to the total number of expected stress cycles in the lifetime of the member.

From the definition of N_T,

$$N_T = \overline{ADTT}(365)\overline{C}\, Y_S \tag{12}$$

where $\overline{ADTT}$ and $\overline{C}$ denote the mean values of random variables ADTT and C. Substituting Eqs. 11 and 12 into Eq. 10 gives:

$$D = \frac{ADTT(365)C}{N_T} \left(\frac{W_{eq} gmih}{\gamma Z_x W_D g_D i_D m_D h_D} \frac{1}{Z_x} \frac{S_{rD}}{S_r}\right)^3 \tag{13}$$

Let:
$G = g/g_D$ (14)
$I = i/i_D$ (15)
$M = m/m_D$ (16)
$W = W_{eq}/W_D$ (17)

$$H = h/h_D \quad (18)$$
$$S = S_r/S_{rD} \quad (19)$$

Equations 14-19 define as random variables the ratio of the true value (random) to the nominal design value.

Substitution now gives:

$$D = \frac{ADTT(365)C}{N_T} \left(\frac{WGIMH}{\gamma Z_x S}\right)^3 \quad (20)$$

Letting the damage accumulation per year be denoted as D, we can express the random variable, Y_F which is the life at which failure actually occurs.

$$Y_F = \frac{X}{D} \quad (21)$$

where X is a random variable accounting for model uncertainty (mainly Miner's law assumption).

Substituting Eqs. 20 into 21 we have:

$$Y_F = \frac{XN_T}{365(ADTT)C} \left(\frac{\gamma Z_x S}{WGIMH}\right)^3 \quad (22)$$

The random variables included in the fatigue life expression contain material terms, Z_X, X and S, truck variables, W, ADTT, H, M, and C and analysis uncertainties I and G. The function given by Eq. 22 is the input to a reliability program. This input must also include statistical parameters and distribution functions of each of the 10 variables discussed in the next section.

4. DATA BASE

In the previous section, the random fatigue life is expressed in terms of random material, loading and analysis variables. Data was accumulated on each of these variables to estimate a nominal value and bias ratio, COV and distribution function. These serve as input to a reliability model to provide consistent design and evaluation fatigue procedures for steel bridges. The data is reviewed herein from a recent report [3]. The data was used to calibrate the reliability procedures by: a) computing safety indices for a range of existing bridges, b) extracting a target safety index, c) selecting a nominal fatigue design and evaluation format and corresponding safety factors (γ) which provide uniform and consistent safety indices over all applications. The same data base is used both in the reliability calculation of existing performance and the selection of the new format values. Hence, small errors in the data base have little or no influence on the final calibration. This would not be the same situation if economic criteria were used to establish the safety indices. Each variable will be separately considered with an assumed lognormal distribution.

4.1 Random Variable M

Although some codes have adopted several of fatigue vehicles, it was decided for simplicity to use only a single fatigue design vehicle. The random variable M, called the moment ratio, reflects the effect of axle spacing and axle weight distribution and is the ratio of the average influence factor due to actual truck spectrum on the bridge to the influence factor of the fatigue design vehicle. Moment ratio varies with span. Truck traffic data from 12 sites were used to calculate the average moment ratios. Data from 5 sites were used to calculate moment ratios for continuous spans. It was found for both simple and continuous spans that the mean or bias of the proposed fatigue design vehicle was reasonably uniform and the COV was about 3%.

4.2 Random Variable W

The random variable W reflects the uncertainty in the estimation of the gross weight of the equivalent fatigue truck. The 54 kip gross weight is obtained from weigh-in-motion (WIM) studies including 30 nationwide sites with over 27,000 truck samples. The value of gross weight is assumed now to be unbiased, although there may be some future growth. A COV of 10 percent is used for the gross weight of fatigue truck in the reliability analysis which implies that there is a 95 percent chance that the effective gross weight of the truck spectrum at a given site will be between 43 kip and 65 kip. This assumption agrees with the results of WIM studies, where effective gross weights in the range of 45 kip to 67 kip were found.

4.3 Random Variable H

The random variable H reflects the effect of multiple presence of trucks on the bridge. Simulating this factor using WIM traffic data for free flow gave a mean value of 1.03 and COV of 0.6 percent.

4.4 Impact Ratio I

The random variable I reflects the uncertainty in estimating the average impact factor for a given site. A mean value of 1.0 and a COV of 11 percent is based on data [3]. Variations from truck to truck within the same site are not important because fatigue is an averaging process and such variations almost cancel out.

4.5 Lateral Distribution Ratio G

The random variable G reflects the uncertainty in the estimation of girder lateral distribution factor. The proposed procedures use the best estimate of the distribution factors. The mean of G is taken as 1.0 with a COV of 13 percent from site-to-site data collected [3].

4.6 Random Variable Z_x

The random variable Z_x reflects the uncertainty in the effective section modulus. In general, the proposed procedures recommend the best estimate of the actual section modulus and, hence, the mean value of Z is taken as 1.0. However, in some specific cases, it is recognized that the effective section modulus is significantly above the actual section modulus because of beneficial effects not normally calculated in design. For example, the effective section modulus is about 15 percent above the actual section modulus for composite sections. Such specific cases are taken care of by increasing the computed section modulus. A COV of 10 percent is assumed for the random variable Z_x.

4.7 Random Variable C

The random variable C represents the equivalent number of stress cycles due to a single truck passage on the bridge. The proposed specification uses the best estimates of C determined from rainflow methods. The coefficient of variation for C, is estimated to be 5 percent.

4.8 Random Variable ADTT

The random variable ADTT represents the true value of the lifetime average daily truck traffic in the shoulder lane. The procedures recommend that the ADTT should be estimated from a site conditions and should be unbiased. Volume uncertainty affects the safety factors much less than stress uncertainty because fatigue damage is linearly proportional to volume but is proportional to the cube of stress range. A 10% COV is used for volume.

4.9 Random Variable S

The random variable S reflects the uncertainty in the estimation of fatigue strength curves. The statistical properties of the random variable S depend on the fatigue category and are obtained from the test results reported from Lehigh University. The mean values and COV of stress ranges at 2 million cycles for different detail categories have been obtained and were used [3].

4.10 Random Variable X

The random variable X reflects the uncertainty in the damage model, mainly due to Miner's Rule. The damage predicted by Miner's Rule is assumed herein to be unbiased. To account for possible test scatter with this rule, a coefficient of variation of 15 percent is used. This value had to be estimated because data on the accuracy of Miner's Rule for welded steel structures were insufficient. This implies there is a 95 percent probability that the predicted life of a specimen using Miner's damage rule will be within 70 percent to 130 percent of the actual life.

5. APPLICATION OF FATIGUE-LIFE RELIABILITY MODEL

In developing and utilizing design procedures, it is normal and appropriate to make conservative assumptions at each step. Many of these conservative assumptions are hidden in various specification parameters and equations. The conservative assumptions are intended to account for uncertainties in each step of the design process by using the most conservative value that could reasonably be expected to occur in that step. Of course, it is highly unlikely that the values for all steps will be at their worst in the same bridge. One of the most important benefits of a reliability analysis is that it shows the interrelationship of the various conservative assumptions that are made at each step in a design or evaluation procedure. For example, in a fatigue evaluation, a larger that expected truck loading may be counteracted by a smaller than expected lateral distribution factor so that the actual life will still exceed the predicted life. Another view of this same analysis is that the overall safety (or fatigue life) can be assured with a very high degree of certainty (say, with a risk of failure of only 10^{-4}) even though the value of the variable in each step is known with much less certainty (say, a 10^{-2} probability level) provided the interrelationship of all variables is properly accounted for in the reliability model. This has an important impact on the overall required safety factor as well as the amount and quality of statistical data needed to produce estimates with high confidence.

The fatigue-life (remaining life) model described above has been applied to many bridge examples . Both the mean life and a safe remaining life based on specified reliability levels have been determined. The calibration of the appropriate safety factor to achieve the described

reliability level is discussed in another paper [4]. The remaining life calculation can be applied in several ways to existing bridges to achieve adequate safety. If an evaluation of an existing bridge reveals that the calculated remaining fatigue life is less than desired, the engineer has four options. First, he could recalculate the remaining life using more accurate data. For example, he could use more accurate calculations of lateral distributions or make a traffic survey to obtain site-specific data on truck volume and weight distribution. Second, he could restrict the weight and/or volume of trucks to increase the fatigue life. Third, he could modify the bridge to improve its fatigue life by a retrofit to improve its fatigue characteristics. Fourth, he could institute periodic inspections to assure that fatigue cracks could be detected before components actually failed. Estimates of the remaining lives of various details have proven helpful in selecting appropriate inspection intervals and allocating inspection efforts.

6. CONCLUSIONS

The reliability model described herein was utilized in developing two recent Guide Specifications adopted by AASHTO [5,6]. One concerns the design of new bridges and the second describes the evaluation of safe lives of existing steel bridges. The derivation of the safety factors is discussed in another paper at the conference [4]. An accurate prediction of the remaining fatigue life of a bridge has important uses. Such an estimate is needed in bridge management systems that are used to make decisions regarding inspection, maintenance, repair, rehabilitation, and replacement of existing bridges. Estimates of remaining fatigue life would also be very useful in assessing the effects of permitting a certain class of overloaded vehicles to use the highways. An example of evaluating the effect of proposed truck weight legislation on fatigue costs is also discussed in the other paper [4].

7. ACKNOWLEDGMENTS

The author acknowledges the contributions of his coworkers on the project, C.S. Schilling and K.S. Raju. Other assistance from I. Friedland, TRB Contract Manager and Project Consultants, Professor John Fisher and Dr. Abba Lichtenstein are appreciated.

REFERENCES

1. Manual for Maintenance Inspection of Bridges, AASHTO, Washington, D.C., 1983.

2. Standard Specifications for Highway Bridges, AASHTO, Washington, D.C., 1983.

3. Moses, F., Schilling, C.G. and Raju, K.S., "Fatigue Evaluation Procedures for Steel Bridges", Washington, D.C., NCHRP 299, Transportation Research Board, 1987.

4. Moses, F., "Safe Life Evaluation of Existing Bridges", IABSE Workshop on Remaining Fatigue Life of Steel Structures, Lausanne, 1990.

5. Guide Specifications for Fatigue Design of Steel Bridges, AASHTO, Washington, D.C., 1989.

6. Guide Specifications for Fatigue Evaluation of Steel Bridges, AASHTO, Washington, D.C., 1990.

Calibration of Load Model for Fatigue Calculation

Calibration d'un modèle de charge pour le calcul à la fatigue

Kalibrierung eines Lastmodelles für die Ermüdungsberechnung

Aloïs BRULS
Lecturer
University of Liège
Liège, Belgium

Aloïs Bruls, born 1941, received his civil engineering degree from the University of Liège in 1965. He is currently a research engineer with the laboratory of the Department of Bridge and Structural Engineering at the University of Liège and a consultant with the company Delta G.C. in Liège.

SUMMARY

This paper explains how it is possible to calibrate a load model for fatigue calculation of road bridges without knowledge of stresses. The accuracy of this simple and efficient method is shown, and initial results are given.

RÉSUMÉ

Cet article expose une méthode qui permet de calibrer un modèle de charge pour le calcul à la fatigue des ponts-routes, sans avoir besoin de connaître les contraintes. La précision de cette méthode simple et efficace est démontrée et les premiers résultats sont donnés.

ZUSAMMENFASSUNG

Der Bericht erklärt, wie ohne Kenntnis der Spannungen die Ermüdungsberechnung einer Strassenbrücke anhand eines Lastmodelles durchgeführt werden kann. Die Genauigkeit dieser einfachen und leistungsfähigen Methode sowie erste Resultate werden vorgestellt.

1. INTRODUCTION

A traffic moving forwards on a bridge induces variable stresses that may produce fatigue damage. A bridge designer needs a load model that allows a stress calculation and a fatigue damage estimation. The question of calibration is to know if the damage produced by a load model is the same as the damage produced by real traffics. This paper considers the following hypothesis :

1° Counting method : the stress spectrum produced by the traffic is converted in a stress-range histogram ($\Delta\sigma_i$, n_i) using the Rain-flow counting method, that does not take in account the mean value [1].

2° Miner Rule : the damage calculation following this method is applicable on all shapes of stress-range histogram and S-N curve [2] :

$$D = \Sigma \frac{n_i}{N_i} \text{ , where,}$$

n_i, is the number of cycles in the stress range histogram ;
N_i, is the number of cycles corresponding to $\Delta\sigma_i$ in the SN curve. That is the number of cycles of a stress range $\Delta\sigma_i$ producing failure.

3° Equivalent stresses range : the total damage produced by a stress-range histogram is replaced by a couple of values ($\Delta\sigma_e$, n_e) that produces the same fatigue damage :

$\Delta\sigma_e$, is the equivalent stress range ;
n_e, is the equivalent number of cycles.

4° Traffic load : using devices measuring axle load of moving vehicles, a high number of recorded traffics are available [3][4][5]. The method developed here under considers two of the more aggressive known traffics.

This paper shows how it is possible to consider equivalent load effects instead of equivalent stress ranges, that allows a calibration comparing equivalent load effects produced by a given traffic and by the model. Such a calibration is then independent of the sizes of the bridges structures.

2. EQUIVALENT LOAD EFFECT

2.1 Damage calculation

For bridge details submitted to fatigue damage some codes define S-N curves [6] [7] [8]. The shape of the existing S-N curves differs following the kind of detail and the codes.
The Eurocode 3 defines mainly an S-N curve with two slopes (Figure 1, curve 3) :

$$N.\Delta\sigma^3 = 5.10^6 . \Delta\sigma_D^3 \quad \text{if} \quad \Delta\sigma \geq \Delta\sigma_D$$

$$N.\Delta\sigma^5 = 5.10^6 . \Delta\sigma_D^5 \quad \text{if} \quad \Delta\sigma_D \geq \Delta\sigma \geq \Delta\sigma_L$$

$$N = \infty \quad \text{if} \quad \Delta\sigma_L > \Delta\sigma$$

Where :
- $\Delta\sigma_D$, corresponding to $N = 5.10^6$, defines the fatigue strength of the considered detail. The part of the curve below $\Delta\sigma_D$ is only applicable by a damage calculation under variable cycles, that is what occurs in bridges ;

- $\Delta\sigma_L$, corresponds to $N_L = 10^8$:

$$\Delta\sigma_L = \sqrt[5]{\frac{5.10^6}{10^8}} \cdot \Delta\sigma_D = 0{,}55 \cdot \Delta\sigma_D \qquad (2)$$

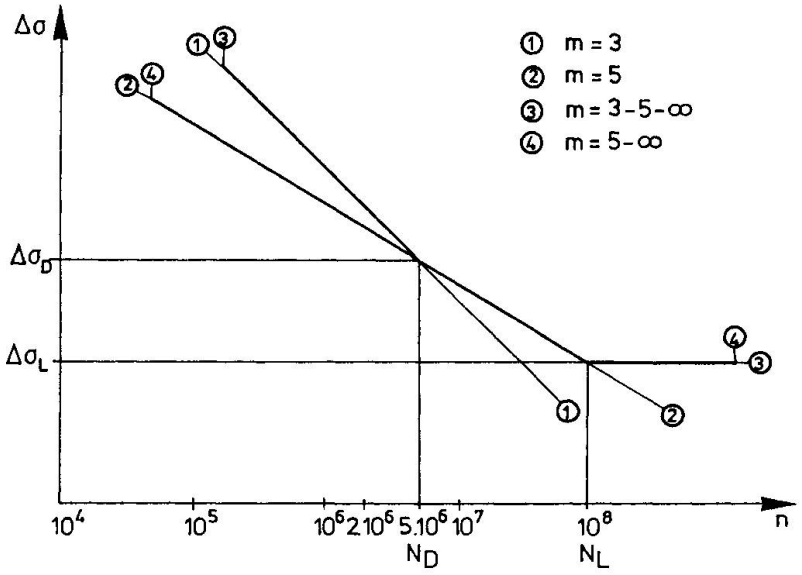

Figure 1 : SN curves

The damage produced by an histogram ($\Delta\sigma_i$, n_i) is expressed by :

$$D_{EC} = \sum \frac{n_i}{N_i} = \sum_{\Delta\sigma_i=\Delta\sigma_L}^{\Delta\sigma_D} \frac{n_i.\Delta\sigma_i^5}{5.10^6.\Delta\sigma_D^5} + \sum_{\Delta\sigma_i=\Delta\sigma_D}^{\infty} \frac{n_i.\Delta\sigma_i^3}{5.10^6.\Delta\sigma_D^3} \qquad (3)$$

The equivalent values must satisfy the relation :

$$D_{EC} = \frac{n_e.\Delta\sigma_e^m}{5.10^6.\Delta\sigma_D^m} \quad , \text{ where } \quad m = 3 \text{ or } 5 \qquad (4)$$

For some kind of details (shear), an other S-N curve is given (Figure 1, curve 4) :

$$N \cdot \Delta\tau_L = 5.10^6 \cdot \Delta\tau_D^5 \quad \text{if} \quad \Delta\tau \geq \Delta\tau_L$$

$$N = \infty \qquad (5) \qquad \text{if} \quad \Delta\tau_L > \Delta\tau$$

Where $\Delta\tau_L$ corresponds to $N_L = 10^8$

The damage is expressed by,

$$D'_{EC} = \sum_{\Delta\sigma_i=\Delta\sigma_L}^{\infty} \frac{n_i.\Delta\sigma_i^5}{5.10^6.\Delta\sigma_D^5} = \frac{n_e.\Delta\sigma_e^5}{5.10^6.\Delta\sigma_D^5} \qquad (6)$$

Other codes [8] consider S-N curves with one slope, and without cut-off (Figure 1, curves 1 and 2) :

$$N \cdot \Delta\sigma^m = 5.10^6.\Delta\sigma_D^m \quad , \text{ where } \quad m = 3 \text{ or } 5 \qquad (7)$$

The damage is expressed by

The equivalent values satisfy the relation :

$$n_e . \Delta\sigma_e^m = \Sigma\, n_i . \Delta\sigma_i^m \qquad (9)$$

In this case, the values $\Delta\sigma_e$, n_e are independent of the fatigue classification of the detail ($\Delta\sigma_D$).

There is an infinity of $\Delta\sigma_e$, n_e values satisfying equation (9) ; some of them are remarkable :

1°) The usual definition considers $n_{en} = \Sigma\, n_i$

and then : $$\Delta\sigma_{en} = \sqrt[m]{\frac{\Sigma\, n_i . \Delta\sigma_i^m}{\Sigma\, n_i}} \qquad (10)$$

2°) We propose to consider $\Delta\sigma_e$ as the centre of gravity of the fatigue damage distribution obtained with an S-N curve with one slope :

$$\Delta\sigma_{em} = \frac{\Sigma\, n_i . \Delta\sigma_i^{m+1}}{\Sigma\, n_i . \Delta\sigma_i^{m}} \quad \text{then :} \quad n_{em} = \frac{\Sigma\, n_i . \Delta\sigma_i^m}{\Delta\sigma_e^m} \qquad (11)$$

As it is shown below this secund definition is less sensible to the slope of the S-N curve and to the cutting of the low stress values.

The fatigue damage distribution considering the load effect histogram (ΔS_i, n_i) instead of the stress histogram is exactly the same if the behaviour of the structure submitted to fatigue is linear : $\sigma_i = C . S_i$.

The equivalent load effects is given by an equation similar to equation (11) where σ is replaced by S. Finally, we propose as definition of the equivalent load effect :

$$\Delta S_{e3} = \frac{\Sigma\, n_i . \Delta S_i^4}{\Sigma\, n_i . \Delta S_i^3} \quad \text{with} : \quad n_{e3} = \frac{\Sigma\, n_i . \Delta S_i^3}{\Delta S_e^3} \qquad (14)$$

If this equation is exact for an S-N curve with one slope corresponding to m = 3, it will be an approximation if other S-N curves must be considered. But the advantage of this definition is that it independed of :

- the sizes of the bridge detail ($\Delta\sigma_i$) ;
- the fatigue resistance of the bridge detail ($\Delta\sigma_D$) ;
- the shape of the S-N curve (m).

It allows a very simple method for calibrating a load model [9]. But before using it, it is necessary to check the differences for other S-N curves shapes and for a lot of levels of the stresse-range regarding the S-N curves. On the other hand, the differences are influenced by the shape of the stress-range histogram. The estimation of these influences is treated below.

3. ACCURACY OF THE EQUIVALENT LOAD EFFECT.

3.1. Load effect histograms.

Considering the bending moment at the midspan in an isostatic beam (L = 10 m.) given by a simulation program [3] [10] [11], the moments produced under a traffic flow are calculated, and applying the Rain flow counting method, a moment range histogram is established (ΔM, n). The Fig. 2 shows the results obtained by two different traffics [5][12] :

a) Auxerre traffic, recorded in France in 1986, that have a high number of high ranges,
b) Rheden traffic, recorded in the Netherlands in 1978 that have a high number of low ranges.

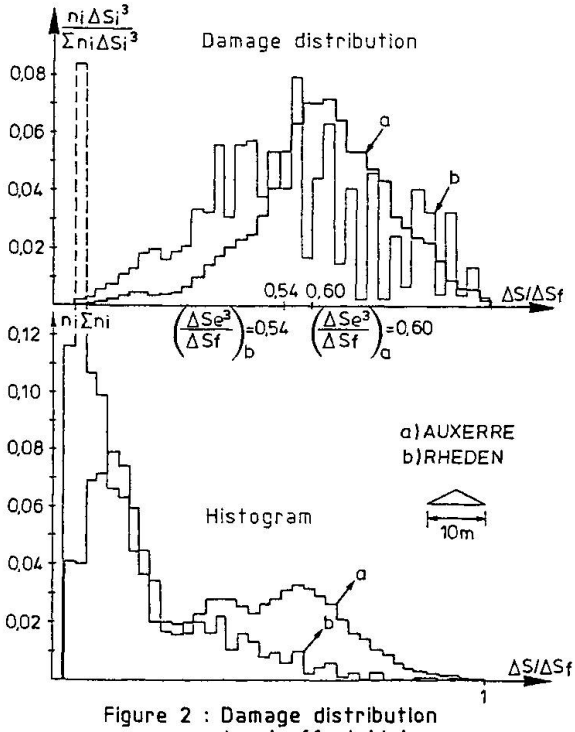

Figure 2 : Damage distribution
Load effect histograms

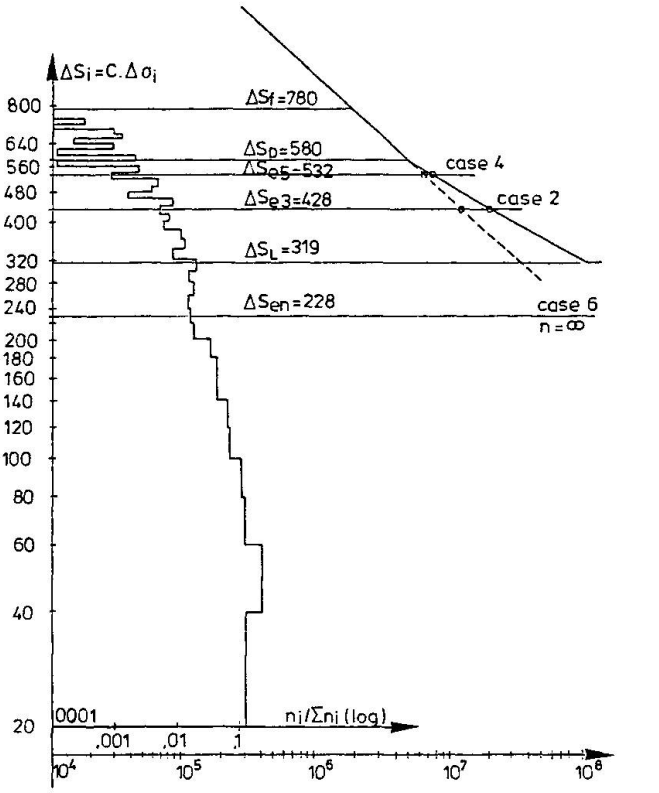

Figure 3 : Fatigue calculation-histogram b : $\Delta S_D/\Delta S_f = 0,7$

These histograms may be considered as representative of all stress range histograms obtained in road bridges under traffic loads.
If the stress is proportional to the moment and if the S-N curve has one slope (m = 3), it is possible to calculate the fatigue damage distribution (Figure 2). In all cases, it appears that the high number of low cycles as well as the little number of high cycles produce low damage. The equivalent load effect defined following equation (14) is situated near the cycles that produces the most damage and is not influenced by the cutting of the high number of low cycles. These two considerations are not applicable by the usual definition of equivalent values (equation (10)).

3.2. Damage calculation.

The fatigue damage is calculated in different cases. In each case, different ratio $\Delta S_D/\Delta S_f$ (load effect corresponding to the fatigue limit/highest load effect) are considered. Following the sizes of the connection the histogram ΔS may be situated differently regarding the ΔS_D value : Figure 3 corresponds to one ratio.

Case 1 : Miner's calculation and Eurocode 3 main S-N curve.

The damage calculation considers the whole ΔS histogram and the S-N curve with 2 slopes of the Eurocode 3 (curve 3). The fatigue damage is expressed by an equation similar to equation (3) :

$$D_{EC} = \sum_{\Delta S_i = \Delta S_L}^{\Delta S_D} \left(\frac{n_i . \Delta S_i^5}{5.10^6 . \Delta S_D^5}\right) + \sum_{\Delta S_i = \Delta S_D}^{\infty} \left(\frac{n_i . \Delta S_i^3}{5.10^6 . \Delta S_D^3}\right) \qquad (15)$$

Case 2 : Proposed equivalent load effect - Eurocode 3 - main S-N curve.
The equivalent load effect ΔS_{e3} is the gravity centre of the fatigue damage distribution calculated with an unlimited S-N curve with m = 3 (curve 1)

$$\Delta S_{e3} = \frac{\sum_{\Delta S_i = 0}^{\infty} n_i . \Delta S_i^4}{\sum_{\Delta S_i = 0}^{\infty} n_i . \Delta S_i^3} \quad \text{then} \quad n_{e3} = \frac{\sum_{\Delta S_i = 0}^{\infty} n_i . \Delta S_i^3}{\Delta S_e^3} \qquad (14)$$

The damage is calculated using the S-N curve with 2 slopes proposed by Eurocode 3 (curve 2) :

$$D_{e2} = \frac{n_{e3} . \Delta S_{e3}^3}{5.10^6 . \Delta S_D^3} \quad \text{if} \quad \Delta S_{e3} > \Delta S_D$$

$$D_{e2} = \frac{n_{e3} . \Delta S_{e3}^5}{5.10^6 . \Delta S_D^5} \quad \text{if} \quad \Delta S_D > \Delta S_{e3} > \Delta S_L$$

$$D_{e2} = 0 \quad \text{if} \quad \Delta S_L > \Delta S_{e3} \qquad (16)$$

Case 3 : Proposed equivalent load effect - S-N curve with one slope (m = 3)
The equivalent load effect is the same as for case 2 : ΔS_{e3}
The damage is calculated by using the S-N curve unlimited with m = 3(curve 1).

$$D_{e3} = \frac{n_{e3} . \Delta S_{e3}^3}{5.10^6 . \Delta S_D^3} \quad \text{in all cases ;} \qquad (17)$$

Case 4 : Modified proposed equivalent load effect - Eurocode 3 main S-N curve.
The equivalent load effect ΔS_{e5} is the center of gravity of the fatigue damage distribution calculated with an unlimited S-N curve with m = 5 (curve 2)

$$\Delta S_{e5} = \frac{\sum_{\Delta S_i = 0}^{\infty} n_i . \Delta S_i^6}{\sum_{\Delta S_i = 0}^{\infty} n_i . \Delta S_i^5} \quad \text{then} \quad n_{e5} = \frac{\sum_{\Delta S_i = 0}^{\infty} n_i . \Delta S_i^5}{\Delta S_e^5} \qquad (18)$$

The damage is calculated using the S-N curve with 2 slopes proposed by Eurocode 3 (curve 3). The equations are similair to equation (16), where ΔS_{e3} is replaced by ΔS_{e5} and n_{e3} by n_{e5}.

Case 5 : Modified proposed equivalent load effect-S-N curve with one slope (m = 3).
The equivalent load effect is the same as for case 4 : ΔS_{e5}.
The damage is calculated using the S-N curve unlimited with m = 3.

$$D_{e5} = \frac{n_{e5} \cdot \Delta S_{e5}^{3}}{5.10^{6} \cdot \Delta S_{D}^{3}} \qquad (19)$$

Case 6 : Usual equivalent load effect - Eurocode 3 - main S-N curve.
The equivalent number of cycles n_{en} is the total number of cycles : $n_{en} = \Sigma n_i$ and the S-N curve is unlimited with m = 3 :
The equation is simular to equation (10)

$$n_{en} = \Sigma n_i \quad \text{then} \quad \Delta S_{en} = \sqrt[3]{\frac{\Sigma_{\Delta S_i = 0}^{\infty} n_i \cdot \Delta S_i^{3}}{\Sigma n_i}} \qquad (20)$$

The damage calculation is made using the S-N curve with two slopes proposed by Eurocode 3. The equation are similar to equation (16), considering ΔS_{en} instead of ΔS_{e3} and n_{en} instead of n_{e3}.

Case 11 : Miner's calculation and Eurocode 3, 2d S-N curve.
The damage calculation considers the whole ΔS histogram and an S-N curve with m = 5 for $\Delta S > \Delta S_L$ (curve 4). The equation is similar to equation 6 :

$$D'_{EC} = \sum_{\Delta S_i = \Delta S_L}^{\infty} \frac{n_i \cdot \Delta S_i^{5}}{5.10^{6} \cdot \Delta S_D^{5}} \qquad (21)$$

3.3. Conclusions.

The accuracy of equivalent load effects as proposed (case 2) is shown on Figures 4 to 6.
Fig. 4 shows that for the histogram obtained in Auxerre :

1°) The damage calculation given by the proposed equivalent values (case 2) is always a little higher than by the application of the Miner's rule (case 1) ; the difference reaches 19 % for $\Delta S_D = 0{,}60\ \Delta S_f$.
2°) If the equivalent values are defined with m = 5 (case 5) instead of m = 3 (case 3), the damage is +/- 15 % lower. Comparing with the S-N curve of the Eurocode (case 1) the damage is +/- 15 % lower if $\Delta S_D < 0{,}60\ \Delta S_f$ (case 5), and a little higher if $\Delta S_D > 0{,}60\ \Delta \sigma_f$ (case 4).
3°) The equivalent value defined for $n_{en} = \Sigma n_i$ (case 6) underestimates very much the damage for $\Delta S_D > 0{,}5\ \Delta S_f$, and gives now damage for $\Delta S_D > 0{,}8\ \Delta S_f$; this definition must be rejected.

Figure 4 : Fatigue calculation

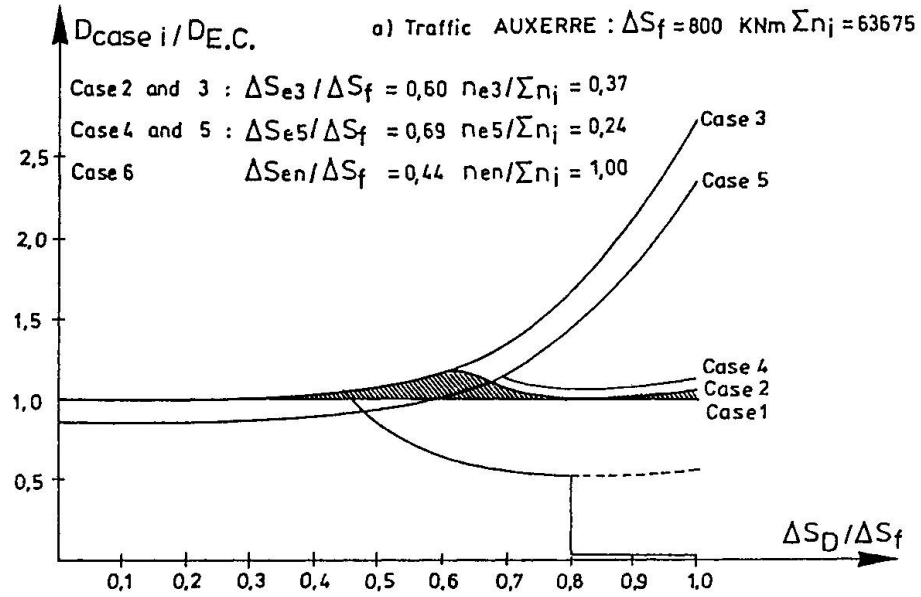

Figure 5 : Fatigue calculation

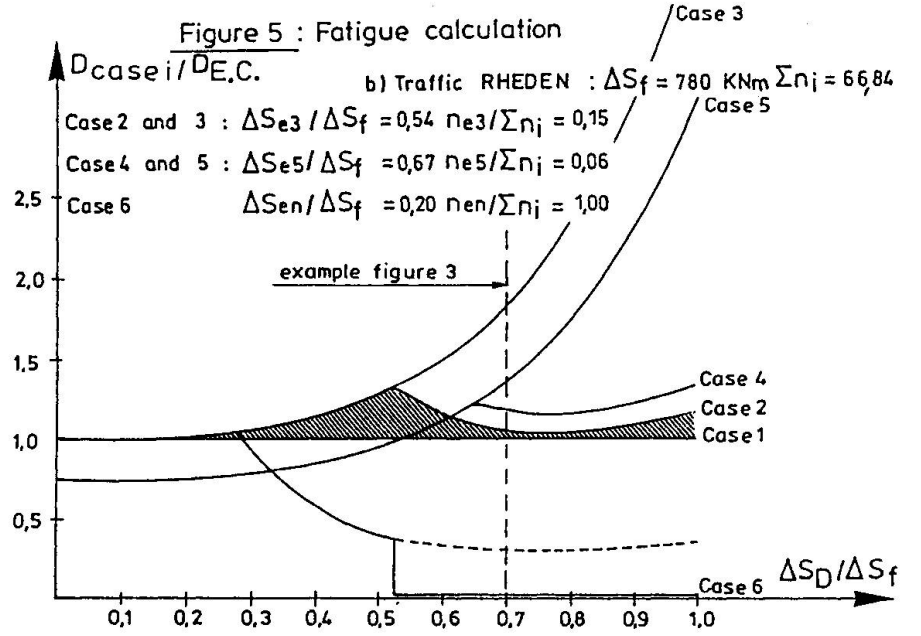

Figure 6 : Fatigue calculation - Eurocode SN curve with 1 slope (m = 5)

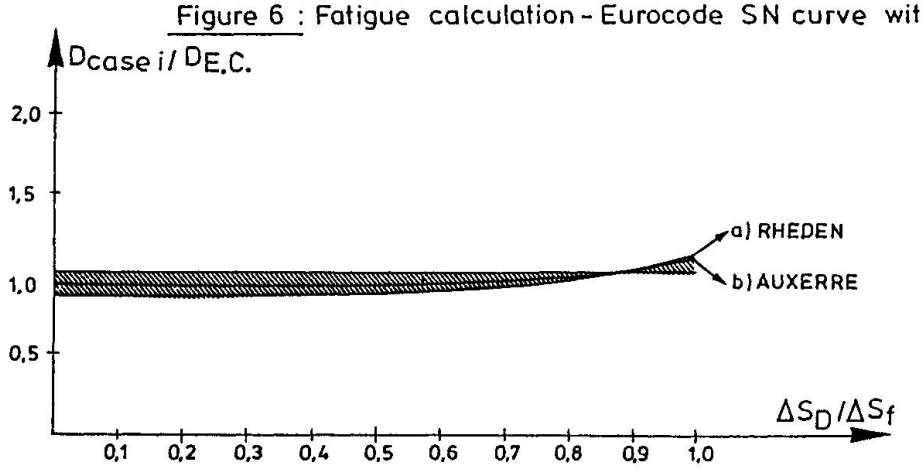

The histogram obtained in Rheden, where exists a higher number of low values, gives larger differences. In this case, the low values represent a high percentage of the total number of cycles but a little percentage of the fatigue damage (Figure 2). The figure 5 shows :

1. The difference between the damage calculation given by the proposed equivalent values (case 2) and by the application of the Miner's rule (case 1) reaches 30 % for $\Delta S_D = 0,54\ \Delta S_f$.
2. The difference between m = 5 (case 5) and m = 3 (case 3) is also higher : 30 %.
3. The value $\Delta S_{en}/\Delta S_f$ is very sensitive to the number of low cycles. In this case $\Delta S_{en}/\Delta S_f = 0,20$ and the damage calculated by this method (case 6) equal zero for $\Delta S_D > 0,52\ \Delta S_f$.

In an other hand, if we treat histograms with high number of high values, the differences between case 1 and case 2 decrease. That has been shown in previous works [9].

If the S-N curve to consider in the Eurocode has one slope (m = 5 for $\Delta\sigma > \Delta\sigma_L$), the difference between the proposed equivalent value (case 2), and a damage calculation, is always lower than 12 % (Figure 6).

After having considered different shapes of histograms, and different positions of these histograms regarding the S-N curves (ratio ΔS_D / ΔS_f or $\Delta\sigma_D$ / $\Delta\sigma_f$), it appears that a load effect defined independently from the bridge details is able to give a damage very close to a complete Miner calculation. The simple calculation gives a higher damage, but the difference is generally lower than 10 %. Only if the stress-range histogram has a very high number of low values (shape b, on Figure 2), the difference reaches 30 % for $\Delta\sigma_D/\Delta\sigma_f$ near of 0,54. On the other hand, as a difference of 30 % in damage means a difference of 9 % in the level of stresses, we may conclude that this method is applicable for the calibration of a simple load model, independently of the bridge behaviour to fatigue.

4. APPLICATION

As the details that are the most sensitive to fatigue are the details influenced by local effects, it is necessary to analyse in a first step effects produced by one vehicle, or one axle.
The equivalent values obtained by the analysis of 20 European traffics are given in the table [5].

	ΔQ_e (kN)	n_e/n_L
One axle	80 - 130	0,80 - 2,40
Tandem axle	150 - 250	0,12 - 0,30
Tandem axle	210 - 260	0,06 - 0,27
Vehicule	330 - 440	0,20 - 0,66

n_L : number of lorries.

The worst case may be covered by a four axles vehicle of 4 x 120 = 480 kN ; with spacings of 1,2 - 4 to 6 and 1,2 m. To check this very simple load model, a set of influence lines representative of real influence lines are simulated with the Auxerre traffic.

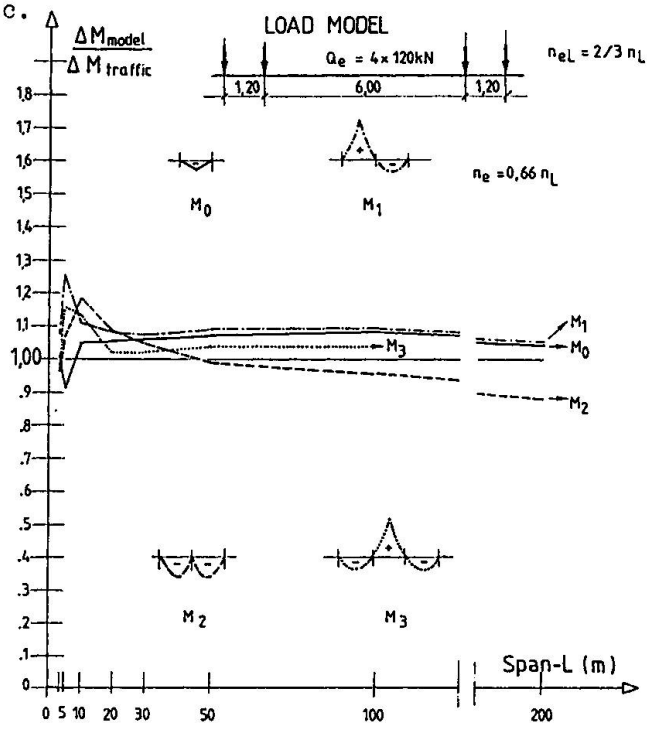

Figure 7

Figure 7 shows that the equivlalent load effects obtained by the simulation are very close to the load effect produced by the simple vehicle. The equivalent load effects is calculated for one equivalent number of cycles obtained by 66 % of the number of vehicles. For short spans (L < 10 m), it seems necessary to examine if a set of vehicle with different geometry is not able to give a better accuracy.
More informations are given in the report for the Eurocode Commission (in preparation).
Comparing these results with previous work [10][11][12][13], it appears that the load of the vehicle of the load model is now higher, because the Auxerre traffic is more agressive; but it is not necessary to consider a complementary distributed load acting simultaneously with the vehicle.

5. CONCLUSION

Figures 4 - 5 and 6 show clearly that the calibration based only on influence lines of load effects, excluding stresses, gives a very good accuracy : the difference reaches exceptionally 30 % in life time, that means 9 % in stress-ranges level. This difference is small regarding the differences between the measured traffics (see table). The definition of a load model in fatigue must consider different types of traffics following the number of lorries expected during a life time ; a difference in the load is perhaps not necessary.
These problems are treated now by the Eurocode Commission and a definitive proposition will be made during this year.
The final aim is to have in a code two solutions for a fatigue verification of road bridge : a very simple load model that gives results on the safe side, and a sophisticated load model that has recourse to a set of vehicles and an computer calculation.

REFERENCES

1. WATSON Dabell, Cycle counting fatigue damage. Society of Environmental Engineers Fatigue Group. 1975.

2. MINER, The accumulation of fatigue damage in Aircraft Materiels and Structures, AGARD agraph n°157, NATO 1972.

3. DE BACK, BRULS, CARRACILLI, HOFFMANN, SANPAOLESI, TILLY, ZASCHEL, Measurements and interpretation of dynamique loads in bridges - 1st phase. ECSC Research report EUR, 1980, pages 1 to 25.

4. HAIBACH, BRULS, DE BACK, CARACILLI, JACOB, KOLSTEIN, PAGE, PFEIFER, SANPAOLESI, TILLY, ZASCHEL,
Measurements and interpretation of dynamique loads in bridges - 2D phase. ECSC Research report EUR 9759, 1985.

5. BRULS, JACOB, SEDLACEK at all, Traffic data of the European countries - Eurocode on actions - Part 12, Traffic loads on road bridges - Working group 2, 1989, pages 1 to 17.

6. Eurocode 3. Design of steel structures - Part 1, E.C.C. 1989.

7. BS 5400, 1980, Steel, concrete and composite bridges. Part 10 - Code of practice for fatigue. Pages 1 to 53.

8. NBN.5 - Ponts en acier - projet 1989 - IBN, Bruxelles, pages 12 à 27.

9. BRULS, POLEUR, Traffic loads on road bridges. Equivalent loads effets - Eurocode on actions - Part 12 - Traffic loads on road bridges - Subgroup fatigue - Appendix 2 - 1989.

10. BAUS, BRULS, Comportement des ponts sous l'action du trafic routier, C.R.I.F. n°MT 145, 1981, pages 1 à 46.

11. BRULS A., Determination des actions pour le calcul des ponts-routes. Colloque A.I.P.C. - Lausanne 1982, pages 865 à 882.

12. BRULS A., Mesures et interprétation des charges dynamiques dans les ponts. 2ème phase - Recherche CECA Rapport EUR 8864 pages 1 à 74, 1984.

13. BRULS A., Eurocode on actions - Part 12 - Traffic loads on road bridges, Preleminary Back ground Documents - Appendix I pages.

Leere Seite
Blank page
Page vide

Loading and Dynamic Behaviour of Bridges

Chargement et comportement dynamique des ponts

Lasten und dynamisches Verhalten von Brücken

Roger GREEN
Professor
University of Waterloo
Waterloo, ON, Canada

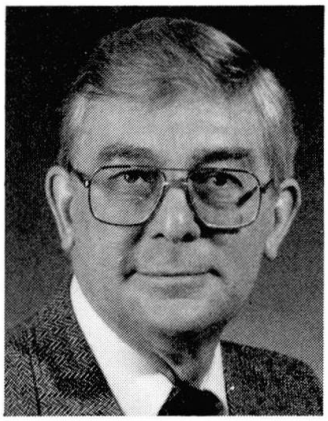

Roger Green, born 1934, holds degrees from London, Queen's-Kingston, Waterloo, and Texas. He has carried out research into bridge behaviour for the past two decades. Topics of interest include dynamics, thermal effects, stability and foundation design.

SUMMARY

Trucks crossing bridges give rise to both static and dynamic effects. This paper describes these effects, including truck-bridge interaction, dynamic response of bridges, and superposition of static and dynamic effects. Modes of vibration are discussed. Recommendations as to how the dynamic response of longitudinal bridge girders may be evaluated are given.

RÉSUMÉ

Les camions circulant sur les ponts provoquent des effets statiques et dynamiques. Cet article décrit ces effets, y compris l'interaction camion-pont, la réponse dynamique des ponts, ainsi que la superposition des effets statiques et dynamiques. Les modes de vibration sont discutés. Finalement, des recommandations sont données dans le but de pouvoir évaluer la réponse dynamique des poutres longitudinales de ponts.

ZUSAMMENFASSUNG

Lastwagen erzeugen beim Überqueren von Brücken sowohl statische als auch dynamische Effekte. In diesem Artikel werden solche Effekte beschrieben, unter anderen die Wechselwirkungen zwischen Lastwagen und Brücke, das dynamische Verhalten von Brücken und die Überlagerung von statischen und dynamischen Wirkungen. Diskutiert werden Formen von Schwingungen. Empfehlungen zur Beurteilung des dynamischen Verhaltens von Brückenlängsträgern werden gemacht.

1. INTRODUCTION

The prediction of the response of bridge structures to traffic load is essential if design or evaluation for fatigue or strength are to be completed with any confidence. Measurement of such response of bridge structures has been an ongoing activity in Ontario for the past 25 years [1-4]. These studies have generally been carried out on short and intermediate span structures and have addressed static, dynamic and bridge-vehicle characteristics.

Most bridge design practice avoids a direct treatment of the dynamic response of superstructures for various vehicular loading conditions. Static force effects of typical traffic or of a design truck are increased to account for bridge-vehicle interaction. Usually the increase is taken as being a function of static load, span length, loaded length and member under consideration [5]. Depth to span ratios may be limited to ensure sufficient static stiffness.

1.1 Basic Requirements

The strength of a structure or component thereof under extreme loads, the ultimate limit state, or moving truck traffic over a defined period, the fatigue limit state, is a function of:

- the resistance of the components or structure
- the static load distribution characteristics of the structure
- the dynamic load distribution characteristics of the structure
- the static load of the truck or trucks
- the dynamic load associated with the truck or trucks
- the dynamic interaction between trucks and structure, present for some structures and frequencies
- the force distribution developed in simple and continuous structures as a consequence of inertia forces.

The resistance of components or structure for a known geometry and displacement history appear to be well established with many stress concentrating geometries known. The S/N resistance relationships for such cases have been documented [6]. Examples are given as Figure 1.

2. THE TRUCK SYSTEM

If a truck travels along a smooth rigid riding surface, the tires will apply a constant force to the surface. This constant tire force is an idealization which will change in the presence of any external force such as wind, braking, steering or pavement undulation. The tire force applied to the surface will have the form of a static force plus a time-dependent force.

As such a truck crosses a bridge, the riding surface will displace and a dynamic interaction between truck and bridge may occur. Thus, the vehicle and superstructure are coupled (Figure 2). The degree of interaction will be a function of the dynamic characteristics of both truck and bridge, and the pavement undulation and discontinuities.

2.1 Static Load Distribution

Recent studies by Hutchinson [7] have considered the distribution of GVW (GV Mass) between axles for bulk haul trucks and tractor trailer combinations. Many of these combinations use an air lift axle which is used when the truck has payload. In general, the measured GVW corresponded to the legal limit.

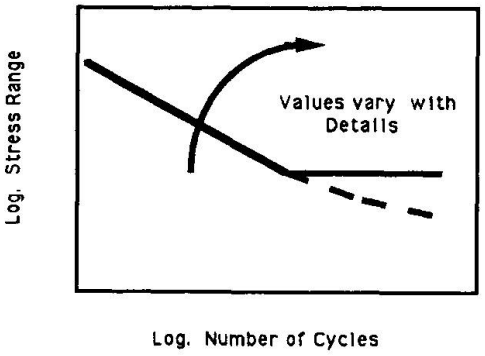

Figure 1 Typical S-N Curve

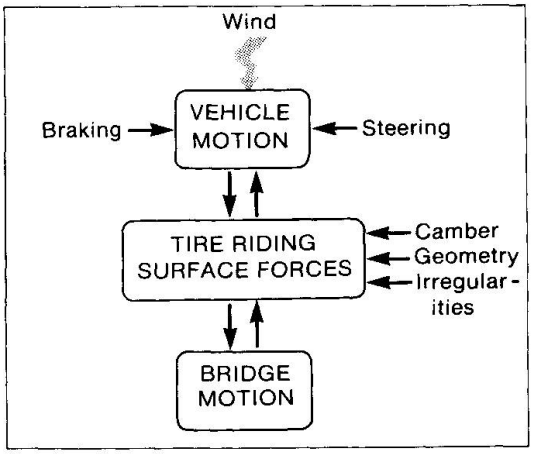

Figure 2 Vehicle-Bridge System

However, axle loads for the rear tandems were greater than the legal limit with values greater than 1.20 of legal being typical. The bending moment due to this uneven distribution of axle load was 1.15 greater than that due to a legal vehicle for spans up to 20 metres. Extreme values of axle load are up to 1.25 times the legal limit for trucks with fixed axles and 1.45 for trucks incorporating air lift belly axles.

The bending moment values resulting from trucks with extreme axle loads are of design significance and may be 40 percent greater than the calculated legal value. The stress range may be 3 times that due to a legal truck. Overloaded trucks are related to the industry being served, the degree of enforcement and the locality. Thus, average truck populations will not be typical in regions of heavy industry.

2.2 Dynamic Axle Loads

Papagiannakis has studied the effects of suspension type, vehicle speed and pavement roughness on the dynamic variation of static vehicle loads[8]. The test vehicle was identical to that used by Woodroffe et al. [9] and allowed change of suspension type and number of axles with relative ease. Used were a walking beam suspension and a multileaf spring suspension in the trailer and tractor, respectively. Typical axle load waveforms are given for leading and trailing axles of the tandem assemblies in Figure 3.

The results given are for pavement conditions and do not include expansion joints or bridge skew. Dynamic load waveforms for tandem axles tend to be in phase and to have similar amplitudes for both walking beam suspensions and leaf spring suspensions. The spectral density of dynamic load indicates that for smooth pavement and modest speed (17 m/sec), frequencies of 3 Hz and 5 Hz dominate and relate to bouncing of the sprung mass on the tires and to wheel eccentricity. Similar data for higher speeds and greater pavement roughness indicate that 3 Hz is the dominant frequency. The standard deviation of axle load is a direct function of suspension type for a given pavement

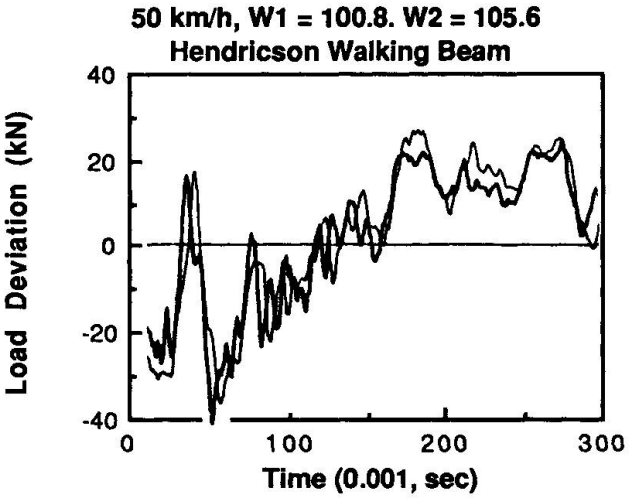

Figure 3 Axle Load Waveforms

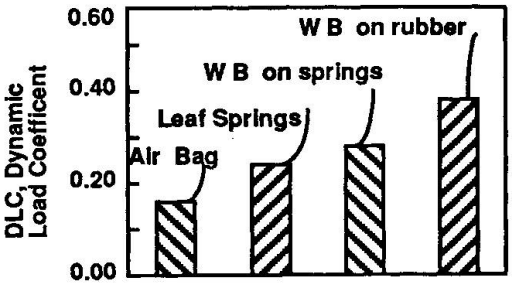

Figure 4 DLC-Various Suspensions

roughness (Figure 4). The deviation indicates that it may be beneficial to modify walking beam suspensions in the interests of reducing dynamic effects. The standard deviation of axle load increases with increasing truck speed and road roughness (Figure 5).

2.3 Ontario Test Data, 1956/7

In 1956/7, a group of 52 bridges known to vibrate were tested using a calibration truck of known weight and free flowing traffic [2]. Only midspan deflection data were obtained. Vibration of the structures indicated a first longitudinal flexural frequency, a forced flexural frequency (2 to 3 Hz), or a first torsional frequency. Dynamic effects tended to be a maximum in the 2 to 5 Hz range. For increasing GVW, the dynamic effects per unit weight decrease for truck length less than span length.

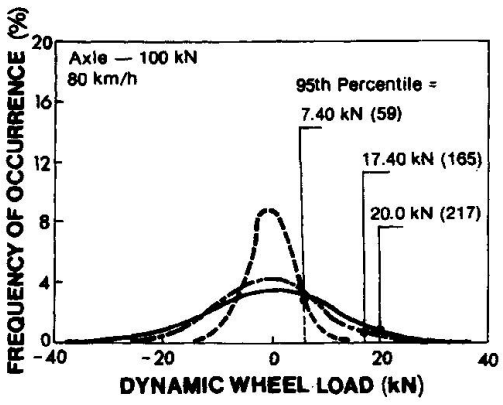

a) Variable Roughness

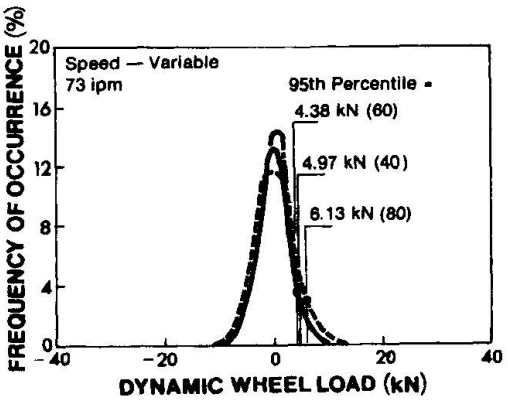

b) Variable Speed

Figure 5 Dynamic Wheel Loads with Variable Roughness and Speed

There was appreciable variation in the dynamic deflection values for a given bridge or between bridges. This variation is due in part to differing pavement roughness and differing bump characteristics, and to the initial conditions of a truck entering the structure. Static span to depth limitations were insufficient to restrict noticeable vibration.

2.4 Ontario Test Data, 1980

Twenty-seven structures were tested using representative test vehicles approaching legal limits (241 kN to 580 kN). Fourteen steel spans of 22 to 122 m, and ten concrete spans of 16 to 41 m were tested. The test procedure and bridge details are given in Reference [1] . Approaches, joints and deck surface were in good condition. The main objective of these tests was to determine the dynamic amplification of main longitudinal members.

2.4.1 Dynamic Characteristics

Between six and 12 nodes of vibration of longitudinal flexure, torsion and transverse flexure could normally be identified for longer span, continuous bridges. All components of the structure resisted the action of static and dynamic load. The transverse static response distribution showed that bracing and barrier walls provide substantial stiffness under the action of a single truck.

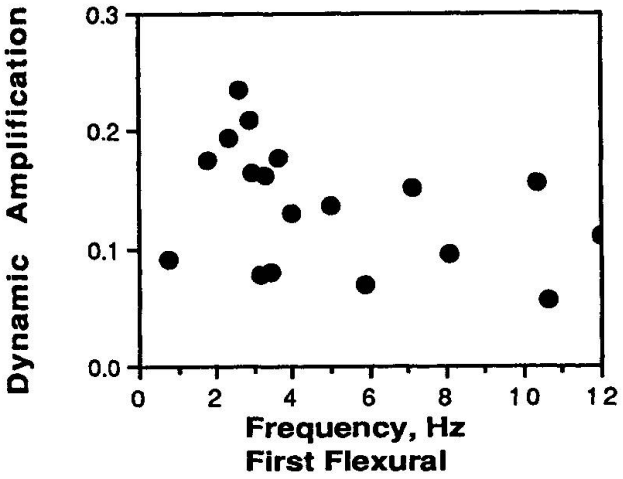

Figure 6 Mean Dynamic Amplification - Frequency

2.4.2 Dynamic Response

Statistical data of dynamic amplification are available. These include all runs by single test vehicles and by other traffic at all speeds in any one lane of each bridge. The mean values of dynamic amplifications are not large (Figure 6) with approximately one-third of the values less than 0.1, and only one-tenth greater than 0.2. Some individual values of amplification, greater than 0.5, were observed. The coefficients of variation are variable and large, with values between 0.56 and 1.11 and a mean of 0.85 for a single lane.

2.4.3 Truck Suspension and Weight

Test vehicles TV1 and TV2 were similar in overall dimensions and weight. TV2 had an air suspension, while TV1 had leaf springs. The mean dynamic amplification due to TV2 was only about 60 percent of that for TV1. The air spring and parallel shock absorber suspension system presumably provides damping under all conditions, whereas the leaf spring assembly will only absorb energy for conditions of large displacement or high rates of loading.

2.4.4 Overall Results

The mean dynamic amplification for all runs generally decreased with an increase in the weight of trucks for spans greater than about 30 m (Figure 7). If the product of truck weight and dynamic amplification is used as a measure of total dynamic load associated with a vehicle, Figure 8 shows the dynamic load corresponding to the data of Figure 7. The dynamic load shown is sensibly

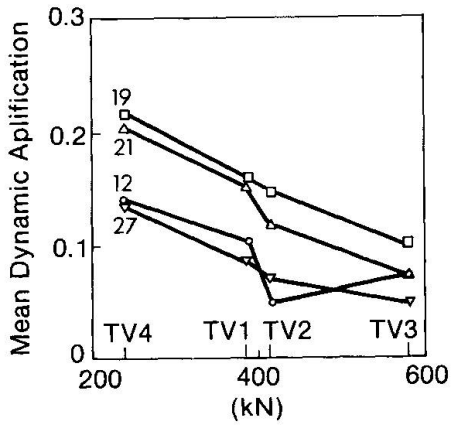

Figure 7 Mean Dynamic Amplification-Weight

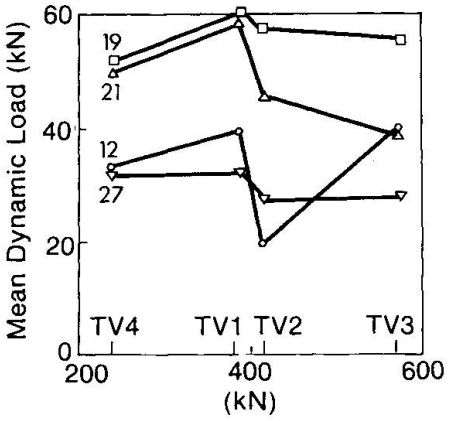

Figure 8 Mean Dynamic Load-Weight

constant with test vehicle weight, with different magnitudes corresponding to different pavement irregularity.

Values of mean total dynamic load for heavy multi-axle trucks have been observed to vary between 30 kN and 120 kN. Perhaps future codes will specify a dynamic load, rather than dynamic load allowance, which is a constant for a wide range of vehicle geometries and loads so reflecting the influence of numbers of axles carrying a load rather than just the total load.

3. LOAD DISTRIBUTION CHARACTERISTICS

3.1 Static Characteristics

The static load distribution characteristics of a bridge cross section are a function of the restraint to distortion. The transverse stiffness of the riding surface (deck) and any transverse bracing will tend to control distortion and hence static load distribution. For example, the static load distribution characteristics to a multibeam structure common in Canada and the United States are shown in the form of transverse influence lines for midspan moment per longitudinal girder in Figure 9. The effect of curbs and cross bracing in improving the load distribution characteristics, (case NM4), is clear.

Also given [10] was a comparison between observed and calculated deflection at midspan. Agreement is good for the shape of the transverse distribution of deflection for finite element models, NM4 and NM2 (not shown). Both these models include vertical cross bracing to minimize distortion. Absolute values of observed and calculated deflection differ, due to a longitudinal restraint at the supports.

3.2 Dynamic Characteristics

In general, the static and dynamic load distribution characteristics of main members of bridge structures are not identical [1]. Deflection-time data from a six girder bridge are shown in Figure 10. For girder 6, a location directly beneath the truck load, dynamic effects are about 60 percent of static. However, for girder 1, static effects are less than the dynamic. The superposition of the transverse static and dynamic effects is given in Figure

11. Interior girders are shielded from the maximum effects of torsional vibration. Such torsional modes will add to the cyclic deformation experienced by any cross bracing.

3.3 Moment Envelopes

The longitudinal distribution of dynamic effects and static effects can be dissimilar. The inertia forces acting on a vibrating continuous beam are proportional to the sum of the products of frequency (squared), the mass, and the modal shape. The magnitude of force is a function of the contribution of a given frequency to the motion of the beam.

Kope [10] calculated the moment envelopes which result when the inertia forces from several modes are assumed to contribute equally, with modal participation proportional to the inverse of frequency squared. Figure 12 shows the distribution of dynamic moment due to self weight and consideration of vibration modes 1 to 4 for a two span bridge beam system. The distribution of moment is nearly uniform throughout the length of the two span system, and has a form quite different from the static effects of traffic load.

Moment envelopes for a two span beam are given in Figure 13. Two forms are used to describe dynamic allowances; one which is proportional to static effects and the second which is a uniform allowance whose magnitude is equal to the maximum design static effect. In positive moment regions little difference exists between the two allowances. However, in moment regions with minimal moment, the dynamic effect due to inertia forces is large in comparison to the static effect.

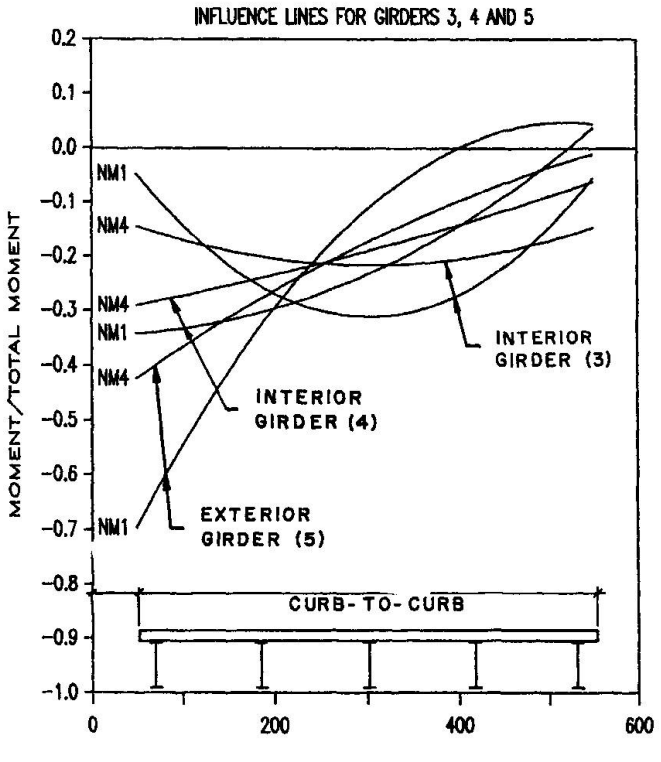

Figure 9 Influence Line for Midspan Moment

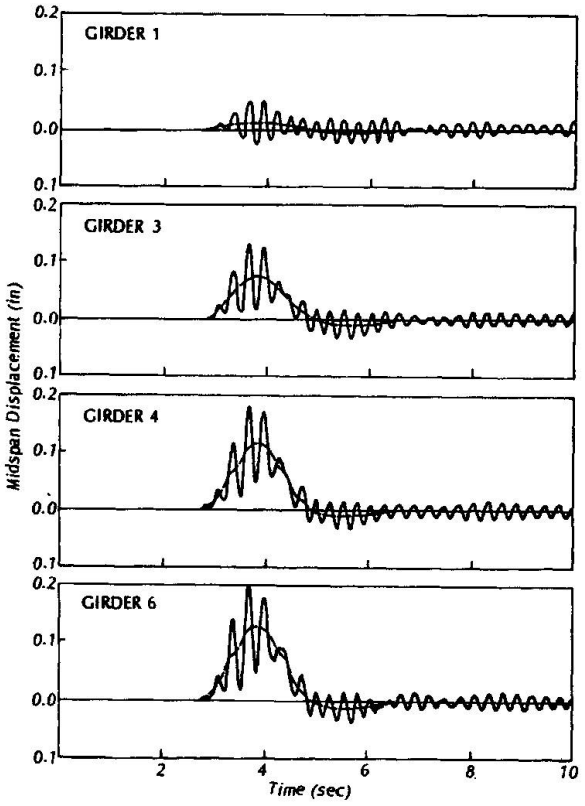

Figure 10 Beam and Girder System

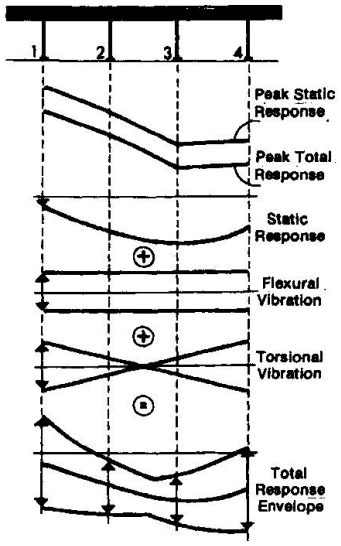

Figure 11 Beam Vibration

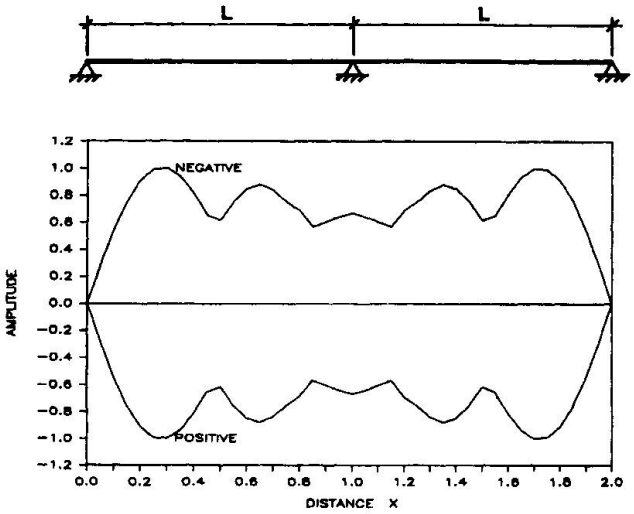

Figure 12 Distribution of Dynamic Moment

3.4 Stress Range

Figure 14 illustrates this effect of enhanced dynamic influence in continuous spans by comparing (a) an observed stress range and (b) a code specified load model stress range. The amplification of the unit positive static effect is 0.2, however, the observed amplification of the negative response of 0.3 is also 0.2. The code model amplification would be of the order of 0.06. Thus, the observed stress range is 1.70 units and code stress range is 1.56 units, a difference worth noting, if the range is raised to either the power of 3 or 5.

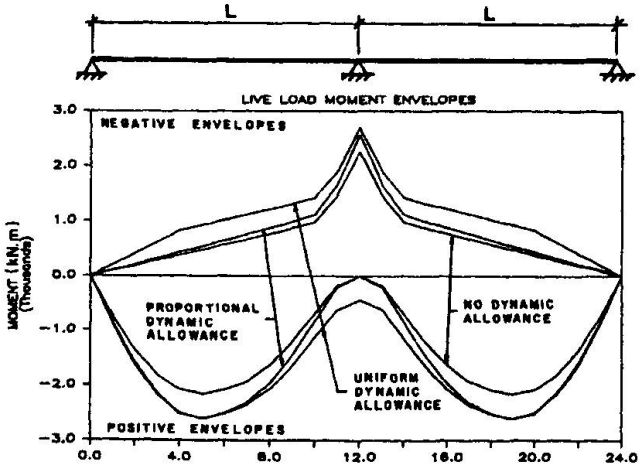

Figure 13 Live Load Moment Envelope

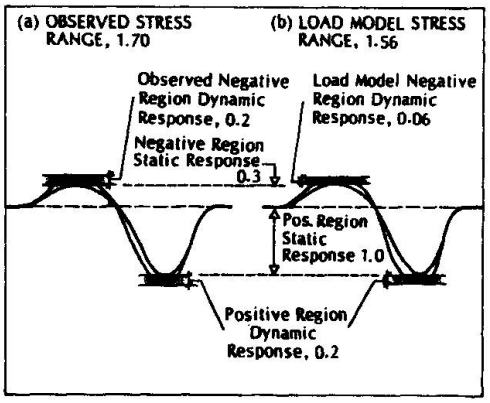

Figure 14 Various Stress Range

3.5 GVW

Results from Ontario studies tend to indicate that the mean dynamic amplification for a given bridge is a function of truck GVW (Figure 15). This implies that dynamic effects per unit weight decrease as the number of axles supporting the load increases for truck lengths less than the span length. The magnitude of such mean values are a function of two main features:

- pavement irregularity
- frequency match between truck and bridge.

For frequency, Billing [1] and Cantieni [11] have shown that dynamic effects do increase over the bridge frequency range of 2 to 5 Hz, a range close to the truck-on-tire frequency. The observed mean dynamic in this frequency range is statistically different to values observed outside the range, and have a global mean which is approximately 50 percent more than for the non frequency match range case.

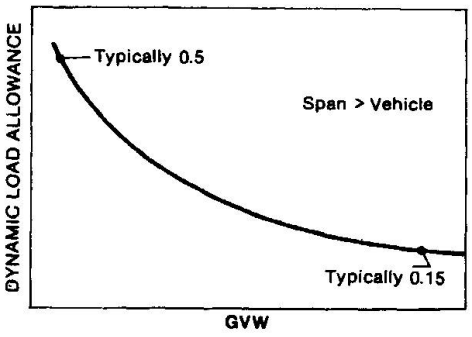

Figure 15 Dynamic Load Allowance - GVW

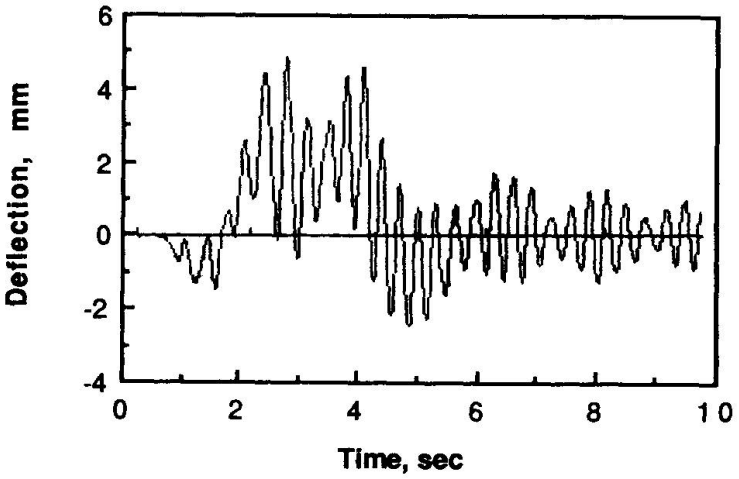

Figure 16 Deflection-time Response Continuous Span

4. STRESS CYCLES

Figure 16 gives the deflection-time trace for the midspan of the second span of a four span prestressed concrete slab bridge, continuous steel structures have similar responses. The two test vehicles each corresponding to legal loads followed each other. This lightly damped response exhibits a number of stress cycles under load and many cycles of free vibration where flexural-torsional beating exists. The results indicate one well defined stress cycle and many minicycles, which, for fatigue considerations, are also damaging and need to be included in any model for fatigue damage.

5. CONCLUSIONS

A truck crossing a bridge results in both static and dynamic effects. The prediction of static stress range in main members and connections can be carried out with ease if the static load distribution characteristics of the bridge superstructure are known. Simple amplification of static effects is a poor predictor of dynamic effects of vehicle load and the interaction of this load with the bridge. The dynamic fraction of vehicle load is a function of pavement irregularity and the lateral position of the vehicle. A frequency match may occur between a vehicle and bridge so amplifying the dynamic wheel

load. Dynamic effects give distributions of force which differ from static effects and are also not proportional to static vehicle load. Load models for fatigue calculation of stress range should consider these dynamic effects.

6. ACKNOWLEDGMENTS

Support for the work reported was provided by the Research and Development Branch, MTO, Ontario, and by the Natural Sciences and Engineering Research Council of Canada. This support is gratefully acknowledged.

7. REFERENCES

1. BILLING, J.R., Dynamic Loading and Testing of Bridges in Ontario. Can. J. Civ. E., V. 11, No. 4, December 1984.

2. GREEN, R., Dynamic Response of Bridge Superstructures - Ontario Observations, Symposium on dynamic behaviour of bridges. TRRL Supplementary Report 275, Transportation and Road Research Laboratory, Crowthorne, Berks, England, 1977.

3. CSAGOLY, P.F., CAMPBELL, T.I. and AGARWAL, A.C., Bridge Vibrations Study, RR 181. Ministry of Transportation and Communications, (MTC), Downsview, ON, 1972.

4. CSAGOLY, P.F. and DORTON, R.A., The Development of the Ontario Highway Bridge Design Code. Bridge Engineering, Vol. 2, TRR 665, TRB, National Academy of Sciences, Washington, D.C., 1978.

5. AASHTO, Standard Specifications for Highway Bridges. 12th Edition, Washington, D.C., 1977.

6. Ontario Highway Bridge Design Code, Code and Commentary. Ontario Ministry of Transportation and Communications, Downsview, ON, 1983.

7. HUTCHINSON, B.G., Private Communication. University of Waterloo, 1989.

8. PAPAGIANNAKIS, A.T., Impact of Roughness-Induced Dynamic Load on Pavement Performance. Ph.D. Dissertation, Dept. of Civil Engineering, University of Waterloo, Waterloo, ON, Canada, 1988.

9. WOODROFFE, J.H.F., LEBLANC, P.A. and LEPIANE, K.R., Effect of Suspension Variations on the Dynamic Wheel Loads of a Heavy Articulated Vehicle. Road and Transportation Association of Canada, Vehicle Weights and Dimensions Study, Technical Report Volume 11, July, 1986.

10. KOPE, B.E., The Static and Dynamic Behaviour of Two Ontario Bridges. M.A.Sc. Thesis, University of Waterloo, Waterloo, ON, Canada, 1986.

11. CANTIENI, R., Dynamic Load Testing of a Two-lane Highway Bridge. Traffic Effects on Structures and Environment, Strbské Pleso, Czechoslovakia, 1987.

Remaining Life of a Suite of Railway Bridges

Durée de vie restante d'une série de ponts-rail

Restlebensdauer einer Reihe von Eisenbahnbrücken

Paul GRUNDY
Assoc. Prof. of Civil Eng.
Monash University
Clayton, Vic., Australia

Paul Grundy gained his BCE and MEngSc at the University of Melbourne, and his PhD at Cambridge, UK. For many years he has pursued research and consulting in remaining life of structures liable to either fatigue at service loads or incremental collapse under repeated overloads.

Gerard B. CHITTY
BHP Melbourne Res. Lab.
Clayton, Vic., Australia

Gerard Chitty gained his BE at the University of Moratuwa, Sri Lanka, and his MEngSc at Monash University. He is currently pursuing research into railway track and bridge dynamics.

SUMMARY
A suite of short span railway bridges in Victoria, Australia, has been investigated for remaining fatigue life. The study revealed that site variability was significant, that a serviceability impact factor less than maximum is needed for estimating fatigue damage, that test data on fatigue strength is scant for the very large number of stress cycles occurring, and that redundancy of load path increases the uncertainty associated with structural response.

RÉSUMÉ
Une série de ponts-rail de petite portée dans l'état de Victoria (Australie) a été examinée du point de vue de leur durée de vie restante. Cette étude a montré que la variation des caractéristiques d'un ouvrage à un autre était déterminante, que le recours à un coefficient d'amplification inférieur aux valeurs maximales était nécessaire pour évaluer le dommage en fatigue, que les données expérimentales sur la résistance à la fatigue étaient insuffisantes pour les très grands nombres de cycles de contraintes rencontrés, et que l'hyperstaticité augmentait l'incertitude quant à la réponse de la structure.

ZUSAMMENFASSUNG
In Viktoria, Australien, wurde eine Reihe von Eisenbahnbrücken kurzer Spannweite hinsichtlich der Restlebensdauer untersucht. Eigene Untersuchungen zeigten, dass die Konstruktionsart für die Ermüdung weitgehend massgebend ist. Zudem stellte sich bei dynamischen Messungen heraus, dass für die Abschätzung der Ermüdungsschäden nicht die maximalen Stosszuschläge angenommen werden müssen und dass mit dem Grad der statischen Unbestimmtheit die Unsicherheit über den Kraftfluss im Bauwerk zunimmt. Die Resultate aus Untersuchungen an einem bestimmten Bauwerk können auf andere Bauwerke ähnlicher Art übertragen werden. Im Verlauf der Arbeiten wurde ein Mangel an Resultaten von Ermüdungsfestigkeitsversuchen im Bereich von kleinen Spannungsdifferenzen festgestellt.

1. INTRODUCTION

The assessment of the remaining fatigue life of a suite of railway bridges requires a variety of data, all of which is subject to some error of estimation and to various levels of confidence. The broad areas of data may be classified as loads, load effects, and fatigue strength. This data is used in a model of fatigue life or fatigue damage which itself is subject to error inherent in simplified engineering models of systems.

In the case of railway bridges of short span, individual axle or wheel loads, their spacing and sequence are important, since a large number of stress cycles can be generated by the passage of a single train. The loading history has to be estimated, as does future loading, where the assumption has been that axle loads and speed will tend to increase.

The load effects of relevance to fatigue life are primarily stress histories at locations where fatigue cracks are likely to develop. The peak stresses depend on two major factors, the influence line (or surface) for the bridge element, and dynamic amplification. The number of stress cycles is also affected by dynamic behaviour.

The fatigue strength, which is subject to inherent uncertainty of estimation due to variability of defects, geometry and materials of fabrication, is also subject to error of detail classification if the detail does not precisely match the detail used in the test programs.

The abovementioned three areas require equal attention if a forecast of remaining life is to lie within acceptable confidence limits. It has been shown [8] that great effort and precision in two of the three areas while neglecting the third will not achieve a confident result. These observations arise out of experience over the past decade in establishing the remaining life for suites of nominally identical railway bridges of approximately 7, 10 and 13 metre spans in Victoria, Australia. All bridges consisted of simply-supported stringers supporting an open unballasted deck or a ballasted non-composite concrete deck. The stringers were made up of taper flange beams with welded coverplates over part of the length. Since construction in 1961 the coverplate terminations have been identified as critical locations for fatigue.

The investigation has been reported [1, 3, 4], and reasonably definitive conclusions reached [6]. However, the work was based upon detailed field measurements at only one site with only one weigh-in-motion station. Recent work has been completed on site dependent factors, which particularly affect the basic influence line and the relationship of impact to speed. Some findings are presented herein.

The initial work was carried out on the shortest span, where calculations revealed the greatest likelihood of fatigue damage. The study was extended to another site with three spans, and then to sites with longer spans. The additional study has provided the information on site dependent parameters.

2. DETERMINATION OF LOADS

2.1 Data Sources

In the context of short span bridges loads are fully defined in terms of axle or wheel load magnitudes *and* spacing. It is quite feasible to reconstruct past or forecast future loads from train consists and timetables. When this method is used to determine loads it is usual to accept manufacturer's specifications of unladen mass, and to assume that the mass is equally loaded on all wheels. For an initial assessment of fatigue damage this data is sufficiently reliable - perhaps more reliable than the data on load effects and on fatigue strength.

When an unfavourable fatigue life prediction is found using paper records to derive loads it often becomes necessary to improve confidence in load estimation by calibration measurements in the

field. Unladen weights of nominally identical locomotives and wagons are found to vary significantly, and often to exceed manufacturer's specifications. Moreover, the distribution of mass over the wheels, particularly for locomotives with six axles, is found to be far from uniform. A previous study [6] found measured masses averaging 11% higher than the estimates provided by the railway authority. (The field measurement is itself subject to error.)

Error in vehicle mass estimation is important for all spans, and unequal distribution of mass to the wheels is important for bridges of short span.

2.2 Measurement Program

A test site was selected at Wallan, 25 km north of Melbourne, where an open deck bridge consisting of three nominally identical simply-supported spans of 6.92 m is located on tangent track. Three complete dynamic weighing stations were established nearby.

The weighing stations followed a well established procedure. They consisted of eight strain gauges fixed to the web of the rail in a segment spanning between sleepers. A flat-topped signal is received while a wheel is within the gauged length. The amplitude gives the wheel load. The weighing station must first be calibrated with a load cell. At speed the flat-topped load signal tends to be headed by a dynamic "spike", and followed by a negative spike. An algorithm which ignores this spike in determining load gives more consistent results.

A test train consisting of a diesel locomotive and two wagons was run many times at various speeds in each direction through the system. Individual wheel loads, midspan flexural stresses, and some stresses at coverplate terminations were recorded. The individual wheel loads, which exhibited considerable scatter, were aggregated into axle, bogie (truck) and vehicle loads. The scatter was significantly reduced at each step.

2.3 Load Measurement Results

The results of vehicle mass measurements are given in Table 1. The ideal weighing station is one which gives the same vehicle mass with negligible scatter, independent of speed. The results are far from ideal. At low speeds the weighing stations give results acceptably close to values established by weighbridge (also subject to error of measurement). With increasing speed apparent mass increased significantly at the first weighing station and decreases significantly at the second. Little change was observed at the remaining weighing station. At any individual weighing station scatter (standard deviation) was limited and did not increase significantly with speed. The variations were more marked for the locomotive than for the wagons.

The results show that dynamic weighing measurements are *speed dependent* and also *site dependent.* An effective calibration would need to be done for speed as well as static load. This calibration would be imprecise because the dynamic effects are different for different locomotives and wagons.

The three weighing sites appeared to be identical, but they were at different distances from the bridge. Since the bridge interrupts the continuity of track modulus properties it can be expected to introduce dynamic effects, but these are impossible to quantify.

3. ESTIMATION OF LOAD EFFECTS

3.1 Analytical Models

All the structures in this study are nominally statically determinate. In design the secondary beneficial effects are neglected, but in review for remaining life they must be considered if an accurate prediction is to be made. Figure 1 depicts a typical influence line for flexural stress in a

simply-supported beam. Field measurements reveal differences which are particularly significant for short spans. The primary reason for the differences in railway bridges is the spanning effect of the track, consisting of rails, sleepers, sometimes ballast, and sometimes timber or reinforced concrete deck [9].

The spanning capability of these elements rounds off the peak of the influence line, and extends the base length. The peak reduction is typically 10% for open deck short spans, and more than 25% for short spans with nominally non-composite reinforced concrete decks. Careful modeling of the secondary elements has achieved compatibility between analysis and measurement [9].

Other sources of stress reduction, which are difficult to model analytically, are dispersion of concentrated loads through the depth of the web, and arching under live load due to friction or seizure of the bearings.

In other field work on cross beams which are assumed to be simply supported on main girders, some degree of end restraint associated with the torsional rigidity of the main girders is always found, leading to a reduction in peak stress.

The extension of base length of the positive component of the influence line, and the extension of a small negative component both contribute to a reduction in fatigue damage. The range of the stress cycle associated with the passage of each wagon is reduced. There is a dramatic reduction in the number of significant stress cycles per train once the base length of the influence line exceeds approximately 1.5 times the clear distance between axles of a typical wagon.

3.2 Site Measurements

Site measurements have been carried out at two levels of sophistication. At the simpler level the measured static peak stress is compared with the analytical prediction. A better understanding of the system is obtained if the influence line is obtained by test. In each case a test train with measured wheel loads is used, and the "static" test is in effect a slow moving test at 5 kph or less, where the position of the train is closely monitored to obtain the influence line.

The use of a train rather than a single axle load makes the determination of the influence line a difficult numerical process, which is sensitive to measurement errors. A single axle loading is not practical, although it has been attempted. With a single axle lifting of the rail away from the point of load application introduces non-linear behaviour which is partially suppressed in practice by neighbouring axles.

Some scatter is always observed on repeated measurement of peak stress or influence line. Apart from errors of measurement the system is in a different state of initial stress after each passage of a train due to the non-linear effects of friction and slip of the bearings and the track system on the beams.

After the static calibration test runs are made at various speeds in each direction to provide statistical data on the effect of speed. It is regrettable that early studies of impact between 1940 and 1960 discarded all the test data except peak values considered significant, thereby losing the statistical properties of impact.

Some of the results at the Wallan site are given in Table 2 and Figure 2. At this site there are three consecutive spans of 6.92 m consisting of a pair of stringers which are taper flange steel joists with welded coverplates. The bridge is open deck (no ballast), and the rail continuously welded on timber sleepers. Effectively the three spans are three sites for the purpose of identifying site dependent parameters.

The results given are the peak stresses recorded at midspan of each girder for each test run, using the test train documented in Table 1. For fatigue damage all stress cycles are significant, but the volume of data and its interpretation is too extensive to report here.

Table 1 - Mass Measurements at Wallan

			All Locations		For Each Loocation					
	Speed kph	No.Runs	Mean A Tonne	Std A Tonne	Mean 1 Tonne	Std 1 Tonne	Mean 2 Tonne	Std 2 Tonne	Mean 4 Tonne	Std 4 Tonne
G523	5	6	127.63	1.64	127.19	1.04	126.66	1.53	129.32	0.94
126.91	10	8	128.56	1.14	128.03	0.51	127.74	0.52	130.14	0.34
	15	5	128.75	0.86	128.32	0.26	128.23	0.41	129.93	0.59
	30	4	127.85	2.96	130.19	1.84	124.92	2.09	128.63	1.55
	60	3	129.76	8.32	141.00	0.90	121.37	1.10	126.90	0.96
	80	2	128.01	10.92	142.04	1.94	115.60	0.83	126.40	0.15
	95	4	126.79	11.53	140.75	2.45	112.92	1.51	126.70	1.86
NOBX	5	6	72.55	0.76	72.64	0.56	72.13	0.89	72.94	0.49
76	10	8	73.09	0.70	73.76	0.61	72.38	0.21	73.15	0.13
	15	5	73.28	0.45	73.00	0.23	73.75	0.13	73.03	0.43
	30	4	72.75	0.94	73.51	0.05	71.75	0.84	73.06	0.32
	60	3	72.22	1.39	74.11	0.14	71.65	0.32	70.91	0.21
	80	2	72.83	0.97	73.76	0.10	71.51	0.12	73.22	0.20
	95	4	74.21	5.40	81.57	1.84	70.24	0.80	70.83	1.37
AOCX	5	6	74.88	0.89	74.62	0.53	74.48	1.01	75.66	0.47
78	10	8	75.69	0.65	75.73	0.46	75.07	0.39	76.38	0.27
	15	5	75.25	0.94	74.97	0.57	74.77	0.83	76.52	0.18
	30	4	74.87	1.14	75.16	0.57	73.88	1.13	75.81	0.56
	60	3	74.62	1.06	76.06	0.34	73.74	0.31	74.06	0.15
	80	2	74.93	0.46	74.77	0.07	74.73	0.51	75.30	0.41
	95	4	74.74	3.06	78.52	1.68	71.88	0.98	73.82	0.99

Table 2 - Peak Stresses (MPa) at Wallan, 6.9 m Span

Speed kph	No.Runs		R1	L1	R2	L2	R3	L3	CPT
0 - 20	19	Mean	41.01	42.75	38.36	40.70	39.56	39.59	36.70
		S.Dev	1.08	0.72	0.87	0.44	0.63	0.36	0.42
30 - 60	6	Mean	42.52	41.44	40.51	41.60	41.53	42.56	36.97
		S.Dev	1.66	0.87	1.17	0.52	0.35	0.67	0.81
80 - 100	7	Mean	47.63	45.42	43.81	43.61	45.68	43.03	41.26
		S.Dev	0.89	1.71	0.62	0.70	1.06	0.72	2.66
All Runs	32	Max	48.80	46.92	44.82	44.58	47.00	43.92	45.66
		Min	38.62	40.34	36.16	39.34	38.62	38.62	36.04
		Mean	42.74	43.09	39.96	41.51	41.33	40.94	37.67
		S.Dev	2.90	1.69	2.37	1.28	2.57	1.68	2.21

Table 3 - Measured Peak Stresses (MPa) at Mangalore, 9.9 m Span

Speed (kph)	No.Runs		Mid 1	Mid 2	Mid 3	Mid 4	CPT 1	CPT 2	CPT 3	CPT 4
0 - 20	17	Mean	29.08	36.06	44.68	25.84	33.68	31.79	45.74	22.71
		S.Dev.	0.59	0.34	0.68	1.30	1.08	2.38	2.03	0.88
30 - 60	25	Mean	30.48	37.57	46.65	28.03	34.87	33.58	47.17	24.95
		S.Dev.	0.55	0.46	1.04	1.44	2.72	4.23	1.53	0.98
80 - 100	9	Mean	33.95	41.03	47.15	34.94	37.89	36.69	50.16	28.30
		S.Dev.	1.47	1.72	6.75	8.61	2.57	3.19	2.51	1.52
All runs	51	Mean	30.63	37.68	46.07	28.53	35.01	33.53	47.22	24.79
		S.Dev.	1.86	1.90	3.15	4.99	2.69	3.89	2.44	2.20
		Max	37.20	44.48	51.90	58.90	42.03	40.82	54.16	30.76
		Min	28.22	35.65	28.49	24.06	30.02	28.49	42.50	21.35

Table 4 - Properties of Fatigue Life Variables

Variable	Mean	Coefficient of variation	Remarks
κ	1.00	0.24	Fatigue strength
α	0.87	0.08	Influence line peak (measured/theory)
ψ	1.11	0.11	Axle loads (measured/estimated)
ϕ	1.19	0.04	Measured impact factor
λ_T	1.16	0.28	Damage per train factor

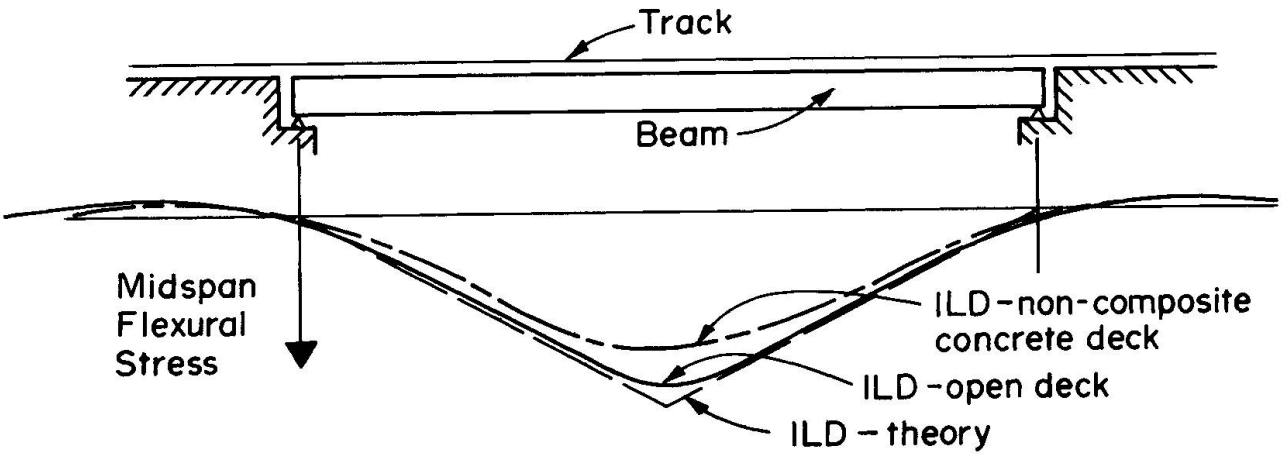

Figure 1 - Influence lines for a simply-supported stringer supporting railway

Further results are given in Table 3 and Figure 3 for a bridge at Mangalore, 110 km north of Melbourne. This is an open deck bridge of three spans of 9.9 m. Each span is supported by four stringer beams in parallel with welded coverplates over part of the span. Table 3 gives the statistical results of 50 test runs with the train consisting of locomotive G523 and wagon NOBX. Half the runs were made with the train headed "up", and half "down". Table 3 gives the stresses at midspan and at coverplate terminations at one end of all four girders in one span. Only the stresses at coverplate terminations are documented in Figure 3.

The results are discussed in the following sub-chapters.

3.3 Site Dependency

Of the six girders monitored at Wallan the highest mean peak stress (all runs) at 43.09 MPa was 7.8% higher than the lowest of 39.96 MPa, shown in Table 2. This is not a surprising result. It is probable that data from other bridges of identical specification would increase the scatter, but this data has not been collected. The scatter revealed by these tests is therefore not a conservative estimate of the scatter to be expected for all similar spans within the railway network.

Sufficient data has been gathered to show that, given the rather small standard deviation on peak stress for any one girder, the difference in mean stress between girders is systematic, not stochastic.

3.4 Effect of Speed

A major gap in design data lies in an impact factor (dynamic increment) to be used for the purposes of estimating fatigue damage. Bridge design specifications give impact factors as a function of speed and span, but these are only suitable for determining peak load effects. Fatigue damage accumulates for all stress cycles, so that the *mean* impact factor provides a more creditable estimate of damage to be expected. The magnitude of the standard deviation of impact factor has only a secondary effect, depending upon the value of the exponent, m, used in cumulative damage calculations.

An idea of the effect of speed can be drawn from Figures 2 and 3. There is apparently a slight dynamic effect at 60 kph compared with crawling speeds - about 4% increment. There appears to be a significant step between 60 kph and 80 kph - about 15% increment compared with crawling speeds. To facilitate this assessment the data have been divided into three speed groups for the two bridges - Slow: 0-18 kph, Medium: 27-66 kph, and Fast: 80-99 kph.

The statistical results appear in Tables 2 and 3. The dynamic increment is also shown. The low scatter in each speed group indicates a fairly reliable estimate of impact.

The impact factor from the AREA Specification for the short span and a speed of 80 kph is 1.58, which is vastly exceeds any values measured here or on any other bridge checked by the authors.

3.5 Redundant Load Paths

With four girders in parallel the bridge at Mangalore can be described as a redundant load path structure. The method of construction is simple, with timber cross members sitting on the four stringers. It is inevitable that the cross-member sits on just two of the stringers until deflection under load brings it in contact with the remainder. Table 3 and Figure 3 show very unequal distribution of load between the stringers, exceeding all expectations. The mean peak stress of the most heavily loaded beam is 47.22 MPa compared with an average of 35.14 MPa. The stresses in the most highly stressed girder at the coverplate termination exceed the constant amplitude fatigue limit, whereas the average peak stresses do not.

The paradox of this result is that redundancy has greatly increased the likelihood of fatigue damage occurring within design life, but not of catastrophic collapse. This poses problems for the owner of the system with limited resources to allocate for inspection of fatigue sensitive details in both redundant and non-redundant load path structures.

4. ESTIMATION OF FATIGUE STRENGTH

4.1 Use of Detail Classification

For fatigue strength reliance must be placed on the detail classes found in structural codes of practice. Information on mean fatigue life as well as design (mean minus two standard deviations) fatigue life is useful if a risk assessment is to be made. However, compromises have been made to present design curves which are simple to use, leading to some inaccuracies.

Some aspects of fatigue strength are still being developed. Two areas of significance are thickness effects and fatigue strength at very high cycles.

Thickness effects are specifically mentioned in relation to welded coverplates. The transition in Detail Class occurs at 25 mm thickness, and the change is sufficient to halve the fatigue life (for exponent, m, equal to 3.0). The coverplates in question have thicknesses of 22 mm and 25 mm, making the interpretation of fatigue strength difficult.

In addition to the thickness question the coverplates overlapped the flanges, and were tapered at the ends, with a continuous fillet weld wrapping around over and under the coverplate. The weld had a leg length of 8-10 mm - small for the thickness of plate.

It was evident that there were enough differences between this detail and those used in laboratory tests for doubt concerning the choice of Detail Class. To improve confidence in predicting remaining life this doubt had to be reduced.

4.2 Laboratory Tests

There is a paucity of test data at very high cycles, exceeding 20 million cycles. For short span bridges more than 100 million cycles of varying amplitude can be expected within the design life. The test data statistics with regard to standard deviation really only apply where most of the test data lie, less than 10 million cycles. It has been reported previously [6, 7, 10] that tests on girders taken out of service provided four new data points in excess of 20 million cycles, one of which was a run out without failure. Even to get these data the Miner's mean stress range was much greater than occurred in practice, with block loadings up to 30% higher than the maximum stress range observed in the field.

The tests were too few in number for statistical inference on their own, but the results were compatible with the higher strength Detail Class (no thickness effect).

The tests were most valuable for two observed phenomena. Firstly, the cracks initiated at the root of the fillet weld and propagated for quite some time through the weld before entering the flange and reducing the effective cross section. Secondly, cracks were clearly visible for more than half the life, and growth rates were virtually identical for all tests. Both observations were important for subsequent analytical modeling of behaviour.

Normally laboratory fatigue tests are too expensive or simply not feasible. In this case the large number of identical bridges at risk justified the investigation.

4.3 Analytical Refinement

When the Detail Class is uncertain a fracture mechanics analysis with finite elements incorporating the quarter point crack tip element will provide useful information - at a cost. The uncertainties surrounding the detail on the bridges investigated prompted the finite element analysis [7, 10]. The result has to be calibrated against the standard detail analysed by the same method.

In this case the analysis found the detail close to the normal coverplate termination in behaviour. It also found that the crack was more likely to grow from an initial defect at the root rather than the toe of the fillet weld.

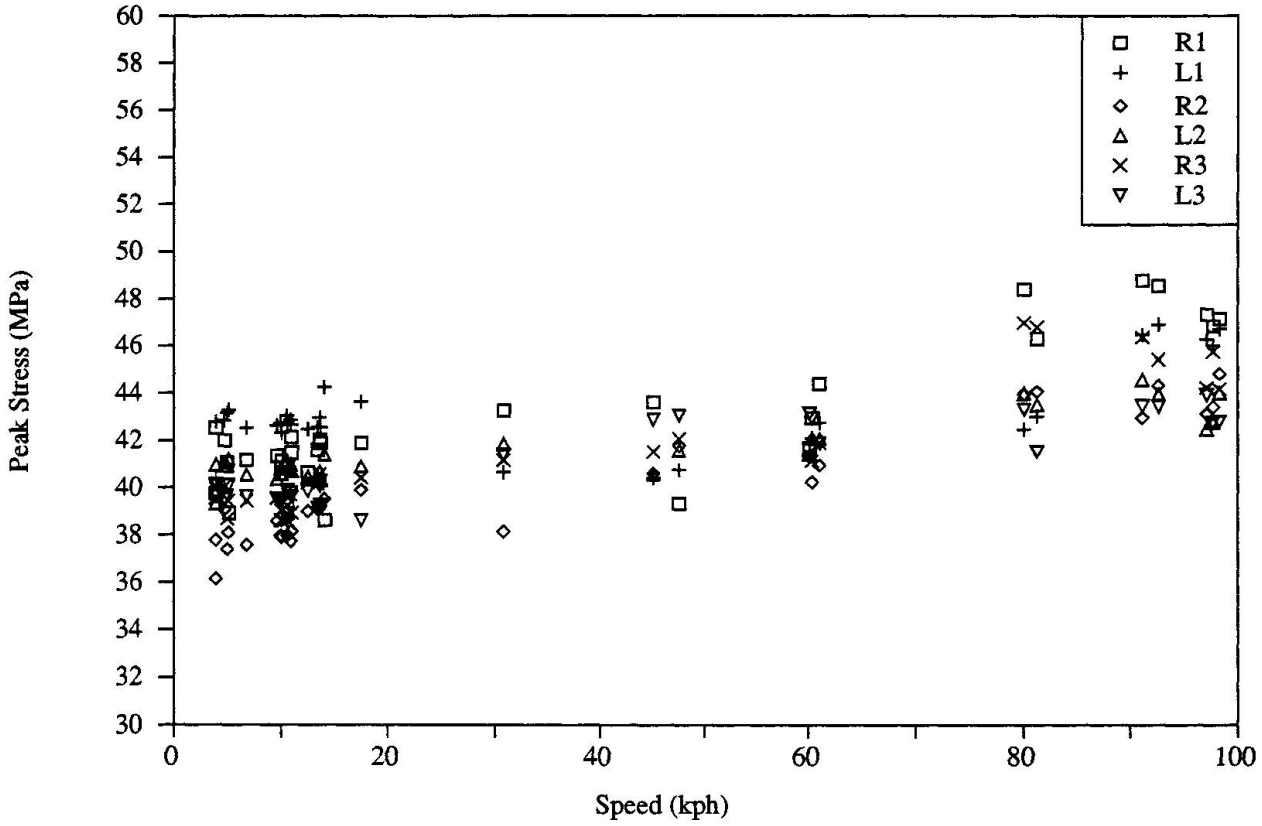

Figure 2 - Midspan stresses on three 6.9 m spans at Wallan

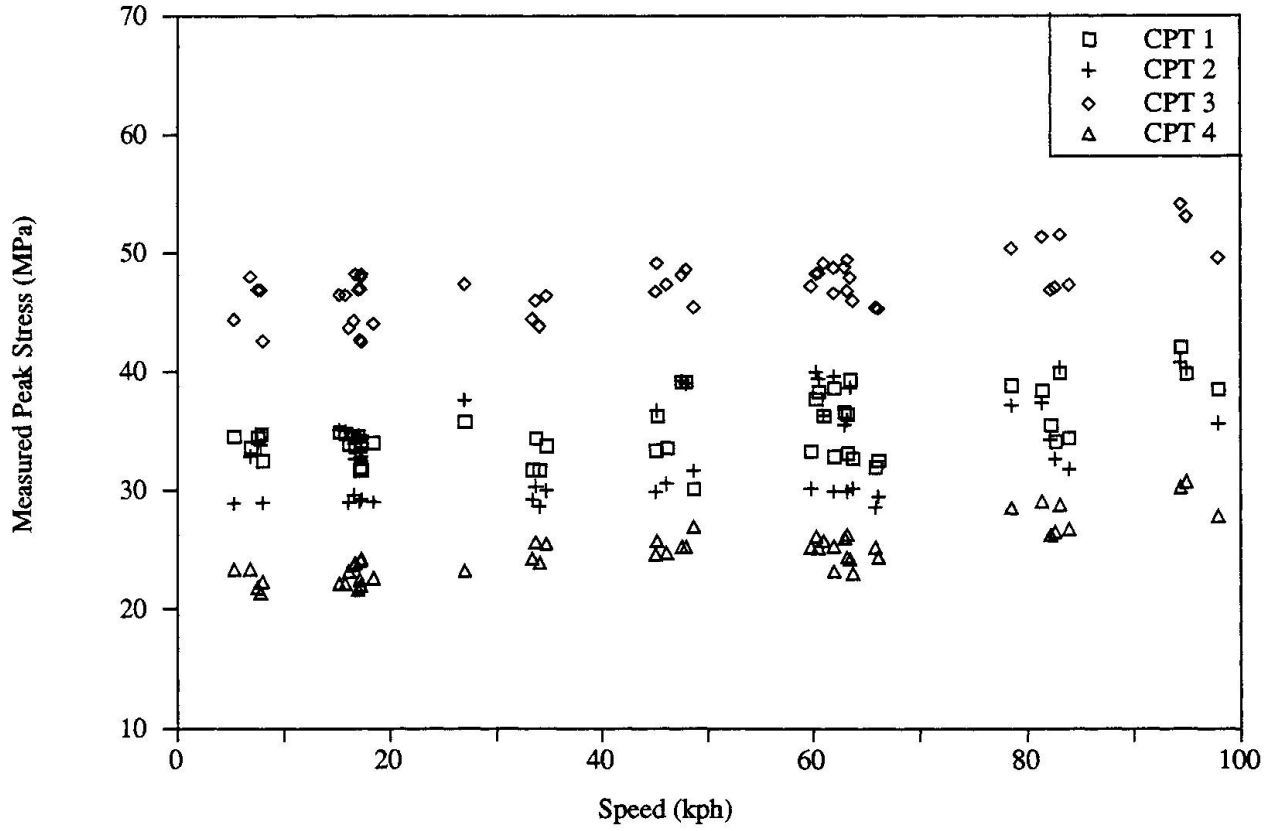

Figure 3 - Stresses at coverplate terminations, 9.9 m span at Mangalore

The fracture mechanics analysis called for an effort comparable to that for the laboratory tests. In normal practice it could only be justified when a detail does not match an existing Detail Class.

4.4 Significance of Detectable Crack Growth Phase

The constant crack growth phase leads to the conjecture that a statistical model assuming normal distribution of life will lead to conservative estimates of a lower confidence limit. It also permits the development of a rational inspection program which will detect damage before it is critical.

5. USE OF SITE MEASUREMENTS

5.1 Verification of Analytical Models

In this study measurements on site were used to establish wheel loads, influence lines and impact factors. Other important phenomena were revealed by site measurements.

Wheel load measurements were useful provided that the effects of speed were recognised and allowed for. Apart from the calibration runs reported herein, the weighing stations were useful for collecting data on regular traffic, which could be related to stress histories on the bridges.

The field measurements of influence lines could be reconciled with improved analytical models. This gave confidence to the determination of influence lines for other short span bridges without the luxury of site measurements.

Although no analytical model of the observed impact factor is available, the value, typically 1.15 for speeds up to 100 kph provides a starting point for assessing fatigue damage of short span bridges similar in character to those which were instrumented. The site measurements revealed that the impact effect was primarily due to the vibration of the bridge in its fundamental mode.

5.2 Direct Prediction of Fatigue Damage

The large scale field measurement program undertaken was justified on account of the large number of structures potentially at risk. It gave an insight into the basic parameters relevant to remaining life, so that rational decisions could be made for the entire system. Such a program would not be economically justified for a unique structure.

A less costly procedure in the case of a unique structure would be to identify the potentially critical locations, to attach strain gauges, and to gather the stress history over a sample period of time. Equipment now exists for cumulative Rainflow analysis of data in real time. This procedure eliminates the need to estimate loads and to calculate load effects. In fact, the uncertainty regarding prediction of fatigue life is reduced at the instrumented site, compared with building a model of response through loads and load effects. This approach, however, does not provide the insights which enable the observations to be applied to other situations without instrumentation.

5.3 Site Dependency

The investigation has clearly demonstrated that at every stage variations in the parameters occur which are associated with the particular site. The parameters are

- axle load distribution
- vehicle mass measurement
- system influence line (surface), i.e., load effect
- dynamic increment versus speed
- notch geometry (weld profile)
- defect type, size and location (for fatigue crack origin).

There are thus two parameters each relating to loads, load effects and resistance, although the last two related to fatigue strength are normally deemed to be allowed for in the statistics of fatigue

strength, and as such are site independent.

6. PREDICTION OF REMAINING LIFE

6.1 Previous Predictions

The predicted life has been the subject of successive refinements [6]. The first estimates were alarmingly short, prompting the field and laboratory testing to replace guesses with measured values. With parameters based on data, and using the more accurate two-slope fatigue strength curve (since most stress cycles were below the constant amplitude fatigue limit), the mean predicted life was 77 years, with a standard deviation of 14 years. This prediction assumes no error in identifying the detail as AREA Category E. This result was based upon the statistical data from field measurements given in Table 4 [6]. In using this data it was assumed that constant amplitude fatigue limit was considered deterministic.

6.2 Revised Predictions

In the light of more recent work on loads, and the discovery that dynamic weighing is speed sensitive, the previously measured wheel load load factor of 1.11 is suspect. If this factor is ignored the predicted mean is increased by 37% for m = 3.0, and 68.5% for m = 5. The latter figure is more likely as the reduction drops most of the stresses into the lower range of the two-slope fatigue life curve.

In addition, with peak stresses now typically 45-55 MPa, and treating the constant amplitude fatigue limit as a variable with the code value a lower confidence limit, a significant number of the details could be free of fatigue damage because the constant amplitude fatigue limit has never been reached.

6.3 Reconciliation with Observed Damage

The structures were put into service in 1961. The need to revise the predicted life is prompted by the observation that, for the 1,422 coverplate terminations on 6.92 m spans on the route in question, not one fatigue crack has been detected after 29 years in service. The apparent conflict between prediction and observation needs to be resolved.

Several explanations are possible. Firstly, the heaviest axle weights were 19 tonnes until 1977, when new locomotives with axle weights 22.5 tonnes were introduced. The chance of not exceeding the constant amplitude fatigue limit before 1977 was quite high. The effective period of damage so far would then be reduced to 12 years.

Secondly, even with the heavier axles, the constant amplitude fatigue limit might not have been exceeded in many cases.

Thirdly, for cracks initiating at the root of the weld, current inspection methods will not discover these until they reach the surface, which takes a large number of cycles.

7. CONCLUSIONS

7.1 Site Dependency

Many key factors affecting stress amplitudes in critical locations for fatigue have been shown to be site dependent. Accurate life predictions will always require some site measurement to obtain acceptable confidence limits to the predictions.

Where a critical detail is repeated at many nominally identical sites sufficient data must be gathered at several sites to quantify site dependent variability.

7.2 High Cycle Life Predictions

Life predictions for bridges are being made for numbers of cycles far in excess of those applied in laboratories to establish fatigue strength curves. Coefficients of variation given for laboratory data can only be applied to structures in service with lives similar to laboratory specimens, typically less than five million cycles. Extrapolation to 50 million or more cycles introduces additional uncertainty.

7.3 Dynamic Effects

A serviceability impact factor is badly needed for estimating fatigue life of bridges, to replace the current ultimate or maximum impact factor. Measured values near 1.15 have been found where the maximum specified by codes is 1.58.

7.4 Redundancy

The greater safety provided by redundant load path structures may be offset by the greater variability of distribution of load between the redundant elements.

REFERENCES

1 Grundy P., Evaluation of Fatigue Life of Some Australian Railroad Bridges. *Colloque Internationale sur la Gestion des Ouvrages d'Art.* Brussels-Paris, 69-74, May 1981.

2 Grundy P., Fatigue as a design Limit State for Bridges. *IABSE Colloquium on Fatigue of Steel & Concrete Structures*, Lausanne, 69-76, March 1982.

3 Grundy P., Fatigue Life of Australian Railway Bridges. *CE Trans. I.E. Aust.*, **CE24**, No. 3, 267-282, 1982.

4 Grundy P., Fatigue Life of Australian Railway Bridges. *IABSE Colloquium on Maintenance, Repair and Rehabilitation of Bridges*, Washington DC. 77-82, September 1982.

5 Grundy P., Fatigue limit state for steel structures. *C.E. Trans. Inst. Eng. Australia*, **CE27**, No. 1, 143-148, February 1985.

6 Grundy P., TEH Soon Heng & Chitty G.B., Measurement versus Estimation of Railway Bridge Fatigue. *Int. Conf. on Measurement and Fatigue*, Engineering Integrity Society, Bournemouth, U.K., 183-199, March 1986.

7 Grundy P. & TEH Soon Heng, Fatigue Strength of Beams at Cover Plate Terminations. *Civil Engg. Trans. I.E.Aust.*, **CE28**, No. 2, 183-189, April 1986.

8 Grundy P., Extending the Life of Bridges. *13th ARRB - 5th REAAA Combined Conference*, Adelaide, 13, Part 6 - Bridges, 163-168, August 1986.

9 Chitty G.B., Effect of Track Continuity and Load Dispersion on the Influence Lines of a Standard 6.88 m Span Railway Bridge, MEngSc Thesis, Monash University, 1985.

10 TEH Soon Heng, Fatigue of Railway Bridges at Coverplate Terminations, PhD thesis, Monash University, 1986.